Title

Influence of soil characteristics and metal(loid)s on antibiotic resistance genes in green stormwater infrastructure in Southern California

Journal

Journal of Hazardous Materials, 424(Pt B)

ISSN

0304-3894

Authors

Hung, Wei-Cheng
Rugh, Megyn
Feraud, Marina
et al.

Publication Date

2022-02-01

DOI

10.1016/j.jhazmat.2021.127469

Peer reviewed

Influence of soil characteristics and metal(loid)s on antibiotic resistance genes in green stormwater infrastructure in Southern California

Wei-Cheng Hung[1], Megyn Rugh[1], Marina Feraud[2], Sumant Avasarala[3], Jessica Kurylo[4], Mathew Gutierrez[1], Karina Jimenez[1], Nhi Truong[1], Patricia A. Holden[2], Stanley B. Grant[5,6], Haizhou Liu[7], Richard F. Ambrose[4], Jennifer Jay[1,*]

[1]Department of Civil and Environmental Engineering, UCLA, Los Angeles, CA, 90095, USA

[2]Bren School of Environmental Science and Management, UC Santa Barbara, Santa Barbara CA 93106, USA

[3]Department of Earth and Planetary Sciences, University of Tennessee, Knoxville, TN 37916, USA

[4]Department of Environmental Health Sciences, UCLA, Los Angeles, CA, 90095, USA

[5]Occoquan Watershed Monitoring Laboratory, The Charles E. Via Jr. Department of Civil and Environmental Engineering, Virginia Tech, 9408 Prince William Street, Manassas VA 20110, USA

[6]Center for Coastal Studies, Virginia Tech, 1068A Derring Hall (0420), Blacksburg, VA 24061, USA

[7]Department of Chemical and Environmental Engineering, Bourns Hall A239, UC Riverside, Riverside, CA 92521, USA

[*]Corresponding author: Jennifer Jay, E-mail: jennyjay@ucla.edu

Abstract

The synergetic effects of metal(loid)s and soil characteristics on bacterial antibiotic resistance genes (ARGs) in green stormwater infrastructure (GSI) has been relatively understudied. Surface soil samples from six GSIs in Southern California over three time periods were assessed for selected ARGs, class 1 integron-integrase genes (*intI*1), 16S rRNA genes, and bioavailable and total concentrations of nine metal(loid)s, to investigate the relationships among ARGs, soil characteristics, and co-occurring metal(loid)s. Significant correlations existed among relative gene abundances (*sul*1, *sul*2, *tet*W, and *intI*1), total metal(loid)s (arsenic, copper, lead, vanadium, and zinc), and bioavailable metal(loid) (arsenic) ($r = 0.29$ to 0.61, $p_{adj} < 0.05$). Additionally, soil texture, organic matter, and nutrients within GSI appeared to be significantly correlated with relative gene abundances of *sul*1, *sul*2, and *tet*W ($r = -0.57$ to 0.59, $p_{adj} < 0.05$). Multiple regression models significantly improved the estimation of ARGs in GSI when considering multiple effects of soil characteristics and metal(loid)s ($r = 0.74$, $p_{adj} < 0.001$) compared to correlation results. Total arsenic was a significant (positive) correlate in all the regression models of relative gene abundances. This work provides new insights into co-dependencies between GSI ARGs and co-occurring metal(loid)s, indicating the need for risk assessment of metal(loid)-influenced ARG proliferation.

Keywords: antibiotic resistance genes; antibiotic resistance; metal(loid)s; co-selection; green stormwater infrastructure

1. Introduction

The widespread occurrence of antibiotic resistance (AR) is a critical global threat to human health (Martínez, 2008). Environmental pathways may play an important role in the emergence and proliferation of AR, especially considering the potential for selective pressure in some settings (Singer et al., 2016). While AR can originate in nature and exist at baseline levels in the environment (Czekalski et al., 2015), anthropogenic pollutants, such as metal(loid)s, can act as stressors and accelerate the development of AR through co-selection of genes and traits that protect both against antibiotics and metal(loid)s (Manaia et al., 2016).

Metal(loid)s are common co-contaminants with antibiotic resistance genes (ARGs) and may co-select for AR by several mechanisms. First, co-resistance occurs when genetic elements conferring resistance to metal(loid)s and antibiotics are linked on the same plasmids or co-occur on the same chromosome. When the presence of metal(loid)s confers selective pressure for plasmid retention, ARGs co-localized on the plasmid are also selected for. Second, cross-resistance occurs when the same mechanism used by the cell for metal(loid) resistance is also effective against antibiotics, such as efflux pumps that remove various metal(loid)s and antibiotics from the cell (Baker-Austin et al., 2006). Third, there can be co-regulation for co-selection, whereby a shared regulatory response for both types of exposure can occur in response to one type of exposure, thereby conferring resistance to the other. All three co-selection mechanisms are similar in that the presence of a stressor may induce indirect selection for bacteria with resistance to multiple chemically-unrelated substances (Baker-Austin et al., 2006). Co-selection of metal(loid)s is expected to depend on the concentrations and speciation of the antibiotics and metal(loid)s in addition to the composition of the microbial community and level of horizontal gene transfer (HGT) (Schlüter et al., 2007). HGT is facilitated by mobile genetic elements (MGEs) and integrons, which

67 can transfer genetic material to a variety of microorganisms (Schlüter et al., 2007). For example,
68 the class 1 integron-integrase genes (*intI*1) are commonly linked to genes conferring resistance to
69 antibiotics and metal(loid)s and serve as an indicator for anthropogenic pollution (Gillings et al.,
70 2015). Genetic transfer, alongside direct and indirect selection for bacteria in metal(loid)-polluted
71 environments, may represent a critical pathway of AR dissemination.

72 Correlations between metal(loid) pollution and AR proliferation have been reported widely,
73 including in effluents and biosolids from wastewater treatment plants (Di Cesare et al., 2016; Gao
74 et al., 2012; Jang et al., 2018; Mao et al., 2015), agricultural soils affected by land application of
75 biosolids or manure waste (Chee-Sanford et al., 2009; Ji et al., 2012), feedlots (He et al., 2016),
76 water bodies impacted by waste discharges (Graham et al., 2011), and metal-spiked experiments
77 in microcosms (Knapp et al., 2011; Stepanauskas et al., 2006; Q. Wang et al., 2020) and in
78 agricultural fields (Hu et al., 2017). In all cases, AR appears to have increased due to metal(loid)
79 co-selection. However, even though urban stormwater and associated surface runoff are known
80 AR reservoirs (Dorsey et al., 2013; Garner et al., 2017) and contain metal(loid) pollutants (Li et
81 al., 2012), green stormwater infrastructure (GSI), such as the stormwater biofilters studied here,
82 has not been evaluated as a compartment for potential AR proliferation.

83 GSI in general, and stormwater biofilters in particular, are designed to capture and treat
84 stormwater runoff as close as possible to where the rain drains. In addition to their primary goal
85 of reducing stormwater flows to streams and lakes, these systems have many additional ecosystem
86 service "co-benefits", including pollutant removal, promoting nutrient cycling (e.g. carbon
87 sequestration, and denitrification), and potentially fostering habitat protection (Askarizadeh et al.,
88 2015; Grant et al., 2013, 2012), and reducing flood risk (Sanders and Grant, 2020). In densely
89 populated Southern California, runoff from both wet and dry weather is a major source of pollution

90 that significantly impacts the regional water quality and poses risks to local health and safety (Ahn
91 et al., 2005; Ambrose and Winfrey, 2015). Urban stormwater runoff has been commonly reported
92 to harbor pathogens and their indicators (Dorsey et al., 2013; Garner et al., 2017; Sidhu et al.,
93 2012). However, although GSI is known to remove contaminants, such as total suspended solids,
94 particulate-associated nutrients (e.g., phosphorous), metal(loid)s, and nitrogen (Blecken et al.,
95 2009) as well as fecal indicator bacteria and human pathogens (Parker et al., 2017; Peng et al.,
96 2016), no studies to our knowledge have assessed their influence on ARGs.

97 Fecal contaminants in stormwater associated with rainfall events are frequently observed to
98 carry elevated levels of antibiotic resistant bacteria (ARB) and antibiotics (Karkman et al., 2019;
99 Powers et al., 2020). Similarly, metal(loid) concentrations tend to be higher during storm events
100 (Li et al., 2012). While antibiotics generally degrade with time in the environment (Cycoń et al.,
101 2019), metal(loid)s are relatively more persistent, although their toxicity can vary depending on
102 oxidation state and complexation with introduced or naturally present organic materials (Hung et
103 al., 2018). In this paper, we hypothesize that, after their initial introduction to GSI media, ARG
104 levels increase due to HGT and co-selective pressure driven by sequestered metal(loid)s,
105 depending on the metal(loid)s' bioavailability and speciation (Isaac Najera et al., 2005). To test
106 this hypothesis we collected field samples and: (1) determined the co-occurrence of ARGs, *intI*1
107 genes, bioavailable metal(loid)s, and total metal(loid)s within GSI soils; (2) examined other factors
108 that potentially contribute to AR, including geochemical conditions, temporal effects, and AR
109 management strategies of GSI soils; (3) performed correlation analysis to investigate the meta(loid)
110 co-selective effects on ARGs within GSI soils; and (4) established multiple linear regression
111 models between gene abundance and a combination of metal(loid) concentrations and soil

characteristics in GSI soils. Such models can further delineate the levels of ARGs and their risk of co-selection by metal(loid)s, providing useful insights for developing and managing urban GSI.

2. Material and methods

2.1. Study area and sample collection

This study took place in Southern California, which is characterized by semi-arid and Mediterranean climates that receive most annual rainfall during winter months (December – March) (National Oceanic and Atmospheric Administration, 2019). Two GSI sites were sampled on each of three University of California campuses (Santa Barbara (UCSB), Irvine (UCI), and San Diego (UCSD)) for a total of six GSI sites (UCSB: Manzanita (MZ) and Sierra Madre (SM); UCI: Culver (CUL) and Verano (VER); UCSD: Altman Clinical and Translational Research Institute (ACT) and Sanford (SAN)). This study took advantage of precipitation being concentrated over the winter months to look at potential changes of ARGs and co-occurring metal(loid)s from the beginning to the end of the wet season. All sites were sampled in the driest part of the year (Fall: October/November 2018), then during the wet season (Winter: February/March 2019), and after the wet season (Spring: April 2019). This study is part of a multi-campus program focused on combating drought by capturing and repurposing stormwater runoff (Pierce et al., 2021; UC Office of the President, 2016).

GSI sites were comprised of both bioswales and biofilters. The land uses surrounding the GSI sites were generally representative of those found across the regional urban landscape (Figure 1 and Table 1). Site size and drainage areas were variable, ranging from 103 to 1,330 m^2 and from 642 to 31,883 m^2, respectively (Figure 1 and Table 1). At each site, soil was exposed by removing aboveground plant materials, rocks, and mulch, and then three soil cores were collected and combined into a composite soil sample of surface soils (0 – 10 cm), using a cylindrical stainless-steel coring cup (5.08 cm diameter x 10 cm length) attached to a slide hammer. The coring cup was fitted with a clean PVC liner, which was replaced between samples. Four soil samples were

collected in this manner at each site, evenly spaced out over the entire dimension of the GSI sites being sampled. Across three time points (Figure S1), a total of seventy-two soil samples were collected. Soil cores were composited in a clean resealable plastic bag after wet-sieving through a brass 2-mm mesh (No. 10) (Advantage Manufacturing, Inc., New Berlin, WI). Sieved soils were subsampled and distributed into separate sterile 15mL Falcon tubes using a sterile scoopula. The Falcon tubes were transported in coolers (4°C) to different laboratories within 6 h for soil characterization, metal(loid) analysis, and ARG analysis.

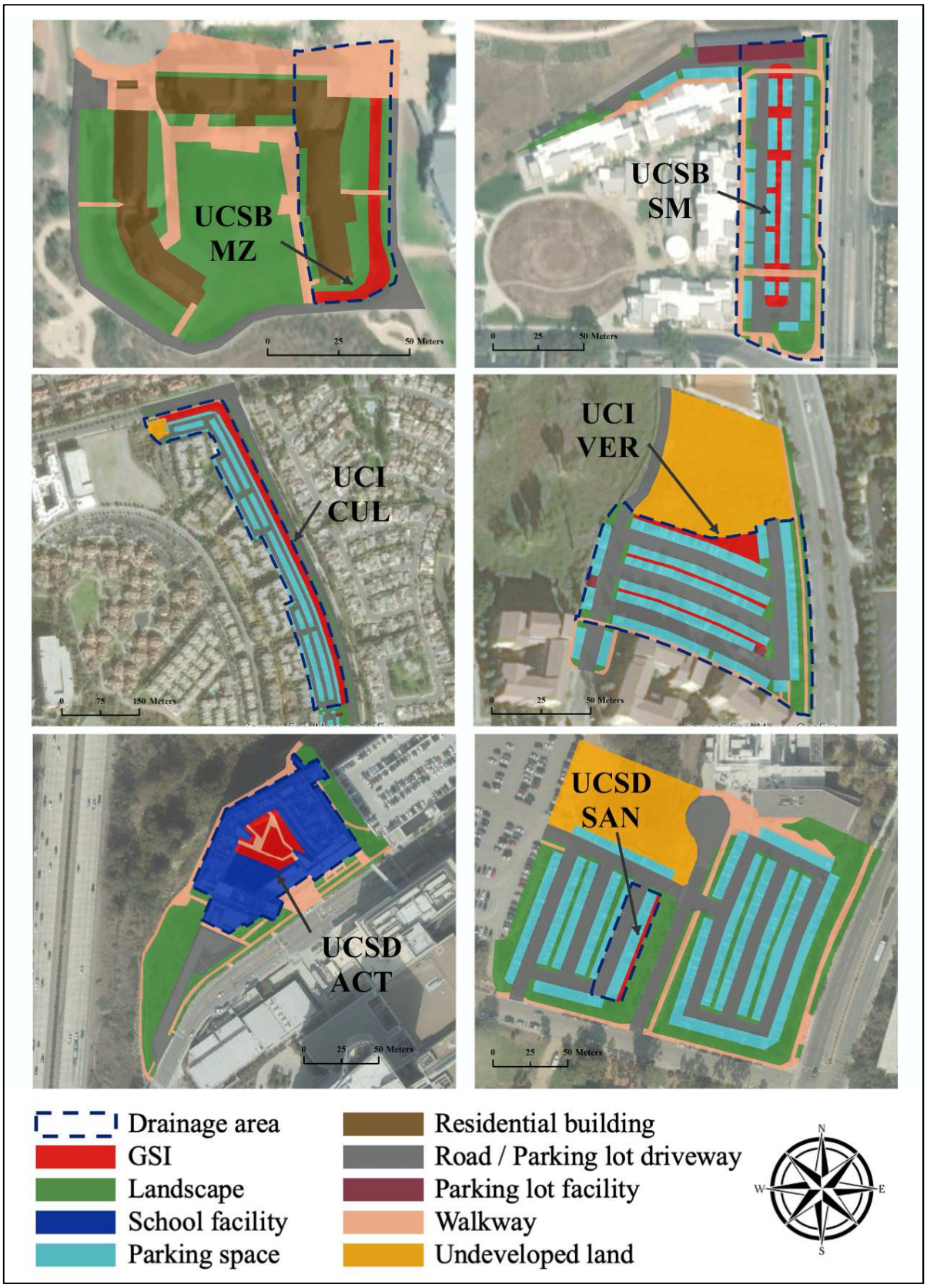
UCSB
MZ
UCSB
SM
UCI
CUL
UCI
VER
UCSD
ACT
UCSD
SAN
0 25 50 Meters
0 75 150 Meters
Drainage area
GSI
Landscape
School facility
Parking space
Residential building
Road / Parking lot driveway
Parking lot facility
Walkway
Undeveloped land
N
W
E
S

144

Figure 1. Land-use types near the six GSI sites sampled in this study, including MZ, SM, CUL, VER, ACT, and SAN at UCSB, UCI, and UCSD, respectively. Dashed areas represent the approximate drainage areas respective to their GSI. Abbreviation: UCSB, University of California, Santa Barbara; UCI, University of California, Irvine; UCSD, University of California, San Diego; MZ, Manzanita; SM, Sierra Madre; CUL, Culver; VER, Verano; ACT, Altman Clinical and Translational Research Institute; SAN, Sanford.

151 Table 1. Site characteristics of Green Stormwater Infrastructure (GSI) distributed in three UC campuses.

	MZ	SM	CUL	VER	ACT	SAN
Campus	UCSB	UCSB	UCI	UCI	UCSD	UCSD
Latitude (N)	34.40916	34.42022	33.64976	33.64571	32.87919	32.88841
Longitude (W)	119.85233	119.87016	117.82472	117.82965	117.22709	117.24468
GSI area (m^2)	363	142	1,330	146	1,024	103
GSI type	Bioswale	Biofilter	Bioswale	Bioswale	Biofilter	Biofilter
Sources of runoff	Residential Building, landscape (lawns), and walkway	Parking lot driveway and parking space	Parking lot driveway and parking space	Parking lot driveway, parking space, and undeveloped land	School facility (AC condensate) and walkway	Parking lot driveway, parking space, and landscape
Impervious drainage area (m^2)	3,978	4,104	31,883	6,405	6,170	642
Year built	2001	2015	2007	2012	2016	2011
Type of irrigation water	RW	RW	RW	PW	PW	RW
Application of soil amendments (or fertilizers)	No	Yes	Yes	Yes	Yes	Yes

152 Abbreviations: MZ, Manzanita; SM, Sierra Madre; CUL, Culver; VER, Verano; ACT, Altman Clinical and Translational Research
153 Institute; SAN, Sanford; NTS, Natural Treatment System; RW, Reclaimed Water; PW, Potable Water.
154
155

2.2. DNA extraction and quantitative Polymerase Chain Reaction (qPCR) of ARGs

For ARG analysis, subsamples were shipped (4°C) to the laboratory at University of California, Los Angeles. Three wet-sieved soil subsamples of 0.25 ± .01 g from each Falcon tube were measured into sterile 2 mL screwcap tubes preloaded with garnet beads and bead solutions (Qiagen, Valencia, CA, USA). Screwcap tubes were stored (-20°C) until DNA extraction. DNA was extracted from archived and thawed GSI soil samples using DNeasy PowerSoil Kits (Qiagen, Valencia, CA, USA) following the manufacturer's instructions. The final DNA extracts were stored at -20°C for quantitative Polymerase Chain Reaction (qPCR). The purity and quantity of total DNA extracts were determined using UV absorption by a Nanodrop 2000c spectrophotometer (Thermo Fisher Scientific, Waltham, MA, USA). DNA extracts were considered as relatively free of contamination from reagents used during extraction as the A260/280 ratio was above 1.8 per the instrument manual.

DNA extracts were analyzed in triplicate for ARGs (*sul*1, *sul*2, *tet*A, *tet*W, and *erm*F), *intI*1 genes, and 16S rRNA genes (a proxy for total cells). These ARGs were chosen as representatives of resistance mechanisms to sulfonamides, tetracycline, and macrolides, respectively, due to the frequent occurrence in garden products (Cira et al., 2021). Each qPCR reaction was conducted in 96-well reaction plates using StepOne Plus qPCR system (Applied Biosystems, Foster City, CA, USA) with a final reaction volume of 25 µL, containing 1.25 µL of each primer, 12.5 µL of PowerUp SYBR Green Master Mix (Applied Biosystems, Foster City, CA, USA), 2 µL of soil DNA extracts (approximately 5–100 ng DNA), and 10 µL of molecular-grade water (Thermo Fisher Scientific, Waltham, MA, USA). Primer concentrations (Table S1) and thermocycling conditions (Table S2) were optimized as described previously (Echeverria-Palencia et al., 2017). DNA standards were designed using sequences from the National Center for Biotechnology

179 Information (NCBI) database and obtained through Integrated DNA Technologies (IDT)
180 (Coralville, IA, USA). Standard curves of the designed DNA fragments were analyzed in triplicate
181 in addition to GSI soil extracts, with the correlation coefficients and amplification efficiencies of
182 the standard curves ranging from 0.991 to 1 and from 86% to 100%, respectively (Table S2). No-
183 template controls (molecular-grade water) were included with each qPCR assay to test false-
184 positive results. The limit of the detection (LOD) for each selected gene (Table S3) were
185 determined following MIQE guidelines (Bustin et al., 2009). Furthermore, soil DNA extracts were
186 spiked with known concentrations (10^3 copies/μL) of targeted DNA standards to examine
187 inhibition effects (Echeverria-Palencia et al., 2017). The specificity of amplified DNA products
188 was further confirmed by melt-curve analysis (Figure S2).
189

2.3. Determination of bioavailable and total metal(loid) content

Subsamples were shipped (4°C) to the University of California-Riverside Water Technology Center laboratory for metal(loid) analysis. Sequential extractions and total acid digestions were conducted using the methods reported by Tessier et al. (1979) and United States Environmental Protection Agency (USEPA) (USEPA, 3050B) (U.S. Environmental Protection Agency, 1996), respectively, to determine the bioavailable (soluble and exchangeable) and total metal(loid) fractions in the soil samples. Briefly, oven-dried soil samples (50°C overnight) were extracted using 1 M $MgCl_2$ at an initial pH 7.0 (25 mL) and shaken at 250 rpm for 2 h at ambient temperature. Solids separated from the supernatants were air-dried for acid digestion. Dried solids were digested on the DigiPrep digestion block (95°C for approximately 3 h in total) using a combination of concentrated nitric acid ([HNO_3], 68%–70% (v/v)) and hydrogen peroxide ([H_2O_2], 30% (v/v)) and diluted to 25 mL with deionized water. Digested samples were diluted to 50 mL with a solution containing 6.8%–7% (v/v) HNO_3, and 0.9% (v/v) H_2O_2. All chemicals were analytical grade or of ultra-high purity (Thermo Fisher Scientific, Waltham, MA, USA), and glassware was acid-washed (1.2 N HCl) and rinsed (deionized water) before use. The concentrations of nine metal(loid)s, including arsenic (As), chromium (Cr), cadmium (Cd), copper (Cu), nickel (Ni), lead (Pb), selenium (Se), vanadium (V), and zinc (Zn), in each extract were analyzed in triplicate with inductively coupled plasma-mass spectrometry ([ICP-MS], 7700 Series, Agilent Technologies, Santa Clara, CA, USA). Total metal(loid)s were calculated by adding bioavailable and acid-digested fractions described above. Internal standard (Ge and Sc), method blanks, and samples with known concentrations were used as quality control measures to assess and correct drifts during the analysis.

213 *2.4. Soil characterization*

214 The prepared soil characterization subsamples were shipped (4°C) to the Analytical
215 Laboratory at University of California, Davis for determination of soil texture, bulk density, cation
216 exchange capacity (CEC), and total nitrogen and total carbon (total N and total C, respectively)
217 using standard methods (Association of Official Analytical Chemists (AOAC), 1997; Rible and
218 Quick, 1960; Sheldrick and Wang, 1993). Gravimetric soil moisture and soil organic matter (SOM)
219 were determined in triplicate by sequential loss on ignition (LOI) at 105°C for 24 h and at 550°C
220 for 4 h, respectively (Gardner, 1986; Nelson and Sommers, 1996). The pH was measured with a
221 pH meter (Oakton Ion 700 benchtop meter, Cole Parmer, Vernon Hills, IL) following the transfer
222 of 10 g of soil into 10 g of deionized water and allowing the mixture to settle for 10 minutes.

223 Additional soil characterization subsamples were transported (4°C) to the UCSB Marine
224 Science Institute Analytical Lab for determination of inorganic nutrients. Soil samples (3 g) were
225 extracted with 30 mL of 2 M KCl solution (Mulvaney, 1996), filtered through Whatman filtration
226 papers (ashless, grade 42, 42.5 μm diameter, Sigma-Aldrich, St. Louis, MO), and analyzed for
227 dissolved nitrate and phosphate using QuikChem8500 Series 2 Flow Injection Analysis system
228 (Lachat Instruments, Milwaukee, WI).

229

2.5. Statistical analysis and geographic information systems (GIS)

Maps of GSI locations and surrounding land uses across three UC campuses (Figure 1) were prepared with ArcMap Version 10.7 (ESRI, Redlands, CA, USA). Most statistical analysis and graphical outputs were performed in R software version 1.4.1 (RStudio Team, 2020). In particular, correlation matrices were performed using the "Hmisc" and "corrplot" packages. Whisker box plots and scatter plots were generated with "ggplot2", "gridExtra", and "ggpubr" packages. Statistical comparisons of ARG levels among soil types were performed using the Kruskal-Wallis test followed by Mann-Whitney U-test for multiple comparisons. Pearson's correlation was used to identify correlations among selected ARGs, metal(loid) concentrations, and soil characteristics. The p-values were adjusted according to Benjamini–Hochberg method in consideration of false discovery rate (Benjamini and Hochberg, 1995). Log-transformed values were used for Pearson correlation analysis since our data were mostly not normally distributed as tested by the Kolmogorov-Smirnov method ($p < 0.05$). Significance was assessed at $p < 0.05$.

Hierarchical cluster analysis (HCA) was performed to identify similarities between total metal(loid)s and bioavailable metal(loid)s using SPSS Version 23 (IBM, Armonk, NY, USA). The distance method and linkage type were based on the Euclidean distance and Ward method, respectively. Although HCA does not require data normality, both total and bioavailable metal(loid)s were log-transformed to yield a more symmetric distribution prior to performing HCA (Templ et al., 2008). Lastly, stepwise multiple linear regression (MLS) was carried out to reveal relationships between relative ARG abundances and environmental factors. The variance inflation factor (VIF) of each input variable was also examined for multicollinearity, variables with VIF higher than three were excluded in the model (H. Wang et al., 2020). ARG abundances and metal(loid) concentrations below the detection limit (BDL) (Table S3 and Table S4) were

253 manually designated at a value of half the detection limits (Helsel and Gilloom, 1986) prior to the
254 analysis.
255

3. Results

3.1. Prevalence and variation of ARGs in GSI in Southern California

In this study, both relative gene abundances (normalized to 16S rRNA genes) and absolute gene abundances (based on total mass of soil) are reported (Table S3), where the former is often used to account for efficiencies during DNA extraction and size of the microbial community (Ji et al., 2012). With one exception, all ARG targets were detected in one or more soil samples collected from the three campuses (Table S3). The *erm*F gene was not detected in any of the soil samples. The relative gene abundances of selected ARGs and *intI*1 ranged from 10^{-7} to 10^{-4} genes per 16S rRNA gene copies (hereafter abbreviated as genes/16S), indicating that *intI*1 and ARGs were represented in approximately 0.00001% to 0.01% of the total soil bacterial 16S rRNA gene abundances.

As noted previously in the Methods, the six GSI sites were sampled from the beginning (October/November 2018), middle (February/March 2019) and end (April 2019) of the wet season to ~~provide~~ indicate both temporal and site-specific variation of abundances of four ARGs and *intI*1 in GSI soils. Across all six sites and all three time points: (1) MZ had the lowest average relative gene abundances of *intI*1, *sul*1, and *tet*W, and (2) ACT contained the highest average relative gene abundances of *intI*1, *sul*1, *sul*2, and *tet*W (Figure 2); however, no significant differences of these genes between locations were observed (adjusted $p > 0.05$). The average relative gene abundances at each site were relatively stable across the three time points with two. First, in MZ and SM, the average relative abundances of *tet*A and *sul*2 genes varied more than an order of magnitude difference between the middle (February/March 2019) and end (April 2019) of the wet season (Figure 2).

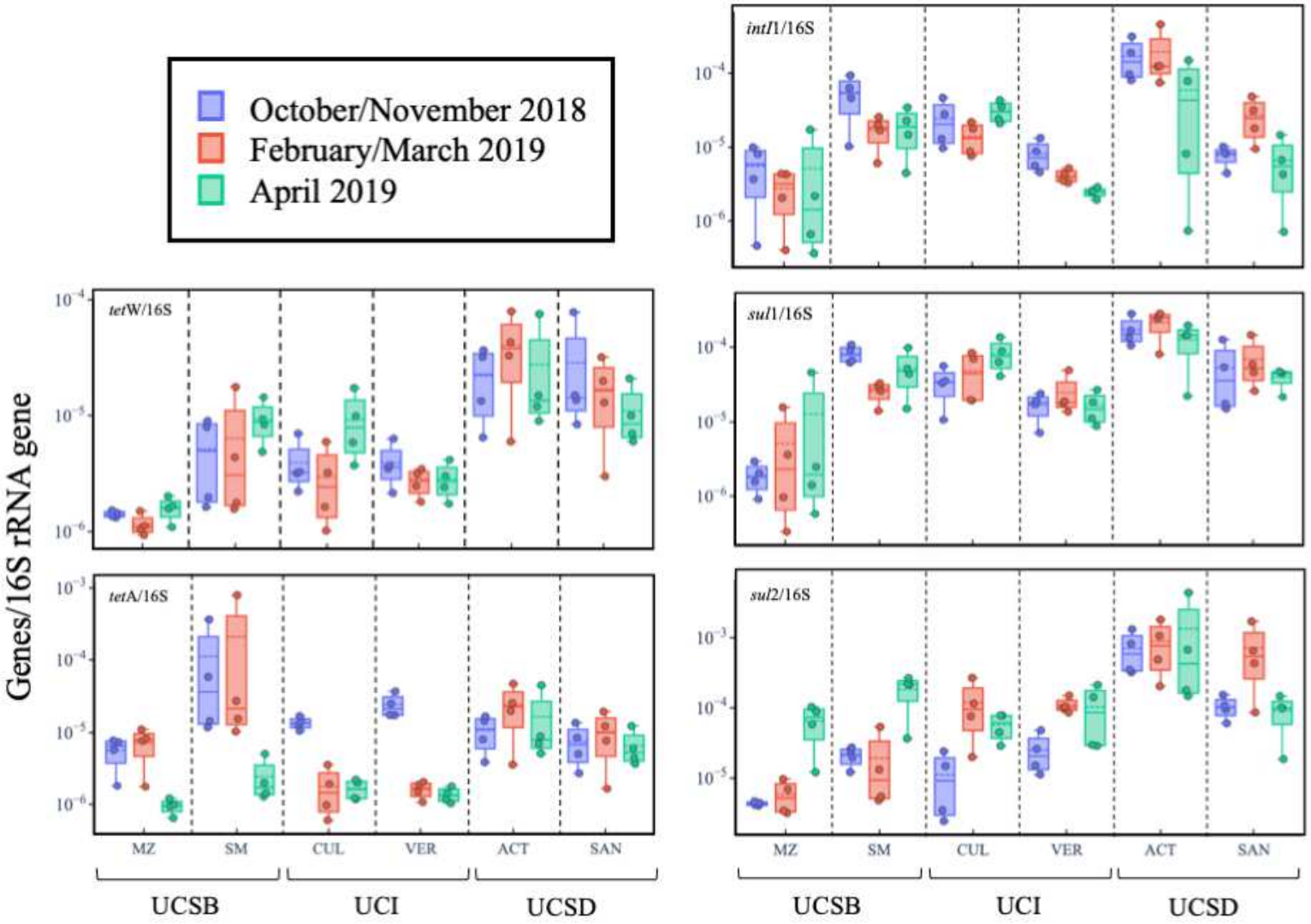
October/November 2018
February/March 2019
April 2019
Genes/16S rRNA gene
intI1/16S
tetW/16S
sul1/16S
tetA/16S
sul2/16S
MZ
SM
CUL
VER
ACT
SAN
UCSB
UCI
UCSD

278

Figure 2. Temporal and spatial variation of the relative gene abundances in six GSI sites in October/November 2018, February/March 2019, and April 2019 (N = 72). The top and bottom boxes represent the 25th percentile and the 75th percentile. The whiskers exclude outliers and extend 1.5 times the interquartile range from both edges of the box. Solid lines and dashed lines are used as medians and means, respectively. Abbreviations: UCSB, University of California, Santa Barbara; UCI, University of California, Irvine; UCSD, University of California, San Diego; MZ, Manzanita; SM, Sierra Madre; CUL, Culver; VER, Verano, ACT, Altman Clinical and Translational Research Institute; SAN, Sanford.

285 *3.2. Bioavailable and total metal(loid)s in campus GSI in Southern California*

286 With a few exceptions of elevated total metal(loid) concentrations, most total metal(loid)
287 concentrations in GSI were similar to naturally occurring background levels (dry soil mass basis)
288 previously measured in surface soils (0–5 cm) in the United States and California (Bradford et al.,
289 1996; Smith et al., 2013) (Table S4) [United States: Pb (25.8 mg/kg), Cd (0.3 mg/kg), Se (0.3
290 mg/kg), As (6.4 mg/kg), Zn (66 mg/kg), Cu (17.9 mg/kg), Ni (17.7 mg/kg), Cr (36 mg/kg), and V
291 (60 mg/kg); California: Pb (23.9 mg/kg), Cd (0.36 mg/kg), Se (0.058 mg/kg), As (3.5 mg/kg), Zn
292 (149 mg/kg), Cu (28.7mg/kg), Ni (57 mg/kg), Cr (122 mg/kg), and V (112 mg/kg)]. Exceptions of
293 elevated total concentrations include Pb (40.9 mg/kg), Cd (5.09 mg/kg), Se (1.30 mg/kg), As (28.8
294 mg/kg), Zn (207 mg/kg), Cu (78.8 mg/kg), Cr (96.8 mg/kg), Ni (83.5 mg/kg), and V (150 mg/kg)
295 measured at several sites. Total As concentrations in most GSI soil samples exceeded screening
296 levels for As in residential areas (0.41 ppm) recommended by California Department of Toxic
297 Substance Control (Cal DTSC) (Cal DTSC, 2020). However, these samples had concentrations
298 below (Cr and Ni) the screening levels for soil metal(loid)s in residential areas recommended by
299 Cal DTSC (Cal DTSC, 2020) (Table S4). Bioavailable metal(loid) concentrations were between
300 2% and 14% of the corresponding total metal(loid) concentrations (Figure S4).

301 The GSI soil concentrations of total As, Cr, Cu, Ni, Se, V, and Zn were highest during the
302 rainy season (February/March) (Figure 3 and Figure S3). In addition, variations in GSI metal(loid)
303 concentrations were also observed across the six sites (Figure 3 and Figure S3). For example, while
304 UCSD exhibited the highest As, Pb, Se, and V concentrations in GSI soils, UCI GSI soils had the
305 highest Cd, Cu, Cr, Ni, and Zn concentrations.

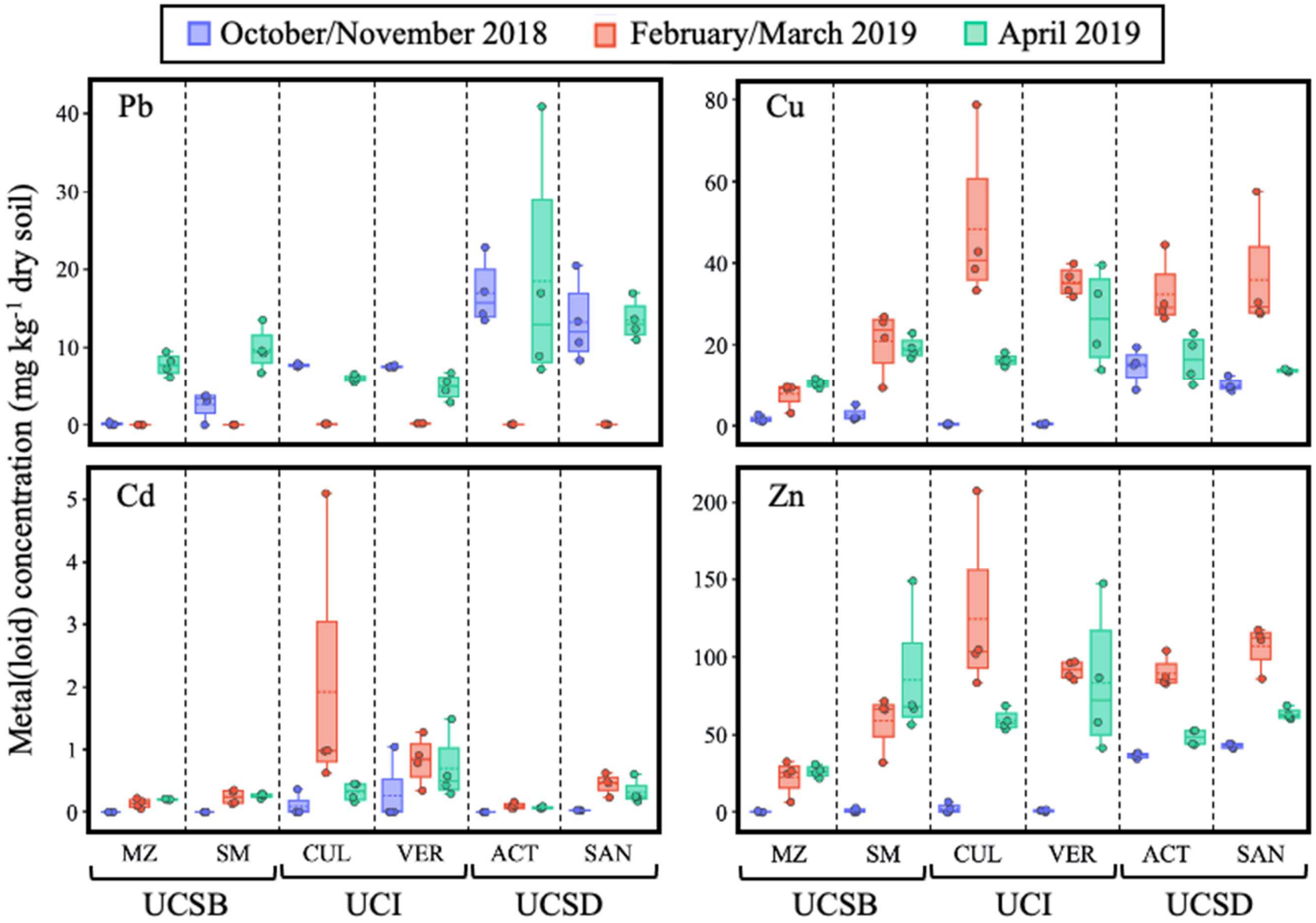
October/November 2018
February/March 2019
April 2019
Pb
Cu
Cd
Zn
Metal(loid) concentration (mg kg-1 dry soil)
MZ
SM
CUL
VER
ACT
SAN
UCSB
UCI
UCSD

306

Figure 3. Temporal and spatial variation of four total metal(loid) concentrations, including copper (Cu), lead (Pb), cadmium (Cd), and zinc (Zn) in six GSI sites. Time points included October/November 2018 (blue), February/March 2019 (red), and April 2019 (green). The top and bottom boxes represent the 25th percentile and the 75th percentile. The whiskers indicate the maximum and minimum points that extend from the 75th percentile and the 25th percentile, respectively. Solid lines and dashed lines are used as medians and means, respectively. Abbreviations: UCSB, University of California, Santa Barbara; UCI, University of California, Irvine; UCSD, University of California, San Diego; MZ, Manzanita; SM, Sierra Madre; CUL, Culver; VER, Verano; ACT, Altman Clinical and Translational Research Institute; SAN, Sanford.

316 *3.3. Correlations between bioavailable metal(loid)s, total metal(loid)s, and ARG abundances*

317 Absolute and relative gene abundances in GSI soils are significantly correlated with many of
318 the log-transformed total or bioavailable metal(loid) concentrations (Figure 4). Absolute gene
319 abundances of *sul*2 and *tet*A were significantly correlated with the following total metal(loid)
320 concentrations: As (*sul*2: $r = 0.34$, adjusted $p < 0.05$; *tet*A: $r = -0.49$, adjusted $p < 0.001$), Zn (*sul*2:
321 $r = 0.41$, adjusted $p < 0.01$; *tet*A: $r = -0.45$, adjusted $p < 0.001$), and V (*sul*2: $r = 0.29$, adjusted p
322 < 0.05; *tet*A: $r = -0.34$, adjusted $p < 0.05$); and Cu (*tet*A: $r = -0.35$, adjusted $p < 0.05$). Additionally,
323 absolute gene abundances of *intI*1/g were significantly negatively correlated with total Cd ($r = -$
324 0.29, adjusted $p < 0.05$).

325 Relative gene abundances of *sul*1, *sul*2, and *tet*W were correlated with total concentrations of
326 As (*sul*1: $r = 0.52$, adjusted $p < 0.001$; *sul*2: $r = 0.59$, adjusted $p < 0.001$; *tet*W: $r = 0.61$, adjusted
327 $p < 0.001$), Cu (*sul*1: $r = 0.29$, adjusted $p < 0.05$; *sul*2: $r = 0.35$, adjusted $p < 0.05$; *tet*W: $r = 0.34$,
328 adjusted $p < 0.05$), and V (*sul*1: $r = 0.38$, adjusted $p < 0.01$; *sul*2: $r = 0.41$, adjusted $p < 0.01$; *tet*W:
329 $r = 0.45$, adjusted $p < 0.001$). Gene abundances of *sul*1/16S and *sul*2/16S were also correlated with
330 total Pb ($r = 0.29$, adjusted $p < 0.05$) and Zn ($r = 0.40$, adjusted $p < 0.01$), respectively.

331 However, absolute and relative gene abundances in GSI soils are only correlated with a few
332 bioavailable metal(loid)s. Relative gene abundances of *sul*1, *sul*2, and *tet*W were significantly
333 positively correlated with bioavailable concentrations of As (*sul*1: $r = 0.33$, adjusted $p < 0.05$; *sul*2:
334 $r = 0.29$, adjusted $p < 0.05$; *tet*W: $r = 0.36$, adjusted $p < 0.01$). Absolute gene abundances of *sul*2
335 were negatively and significantly correlated with bioavailable Cr concentrations ($r = -0.36$,
336 adjusted $p < 0.01$).

337 Total metal(oid)s clustered into three major groups as shown in HCA (Figure 5a): (1) Cu, Cr,
338 Ni, V, Zn, and As; (2) Pb; (3) Se and Cd. In parallel, bioavailable metal(loid)s revealed different

clustering patterns: (1) Cu, Cr, Pb, and Ni; (2) Cd, Se, and Zn; (3) As and V (Figure 5b). Metal(oid)s including Zn, Cu, Cr, and Ni serve as micronutrients in various physiological functions of biological cells.

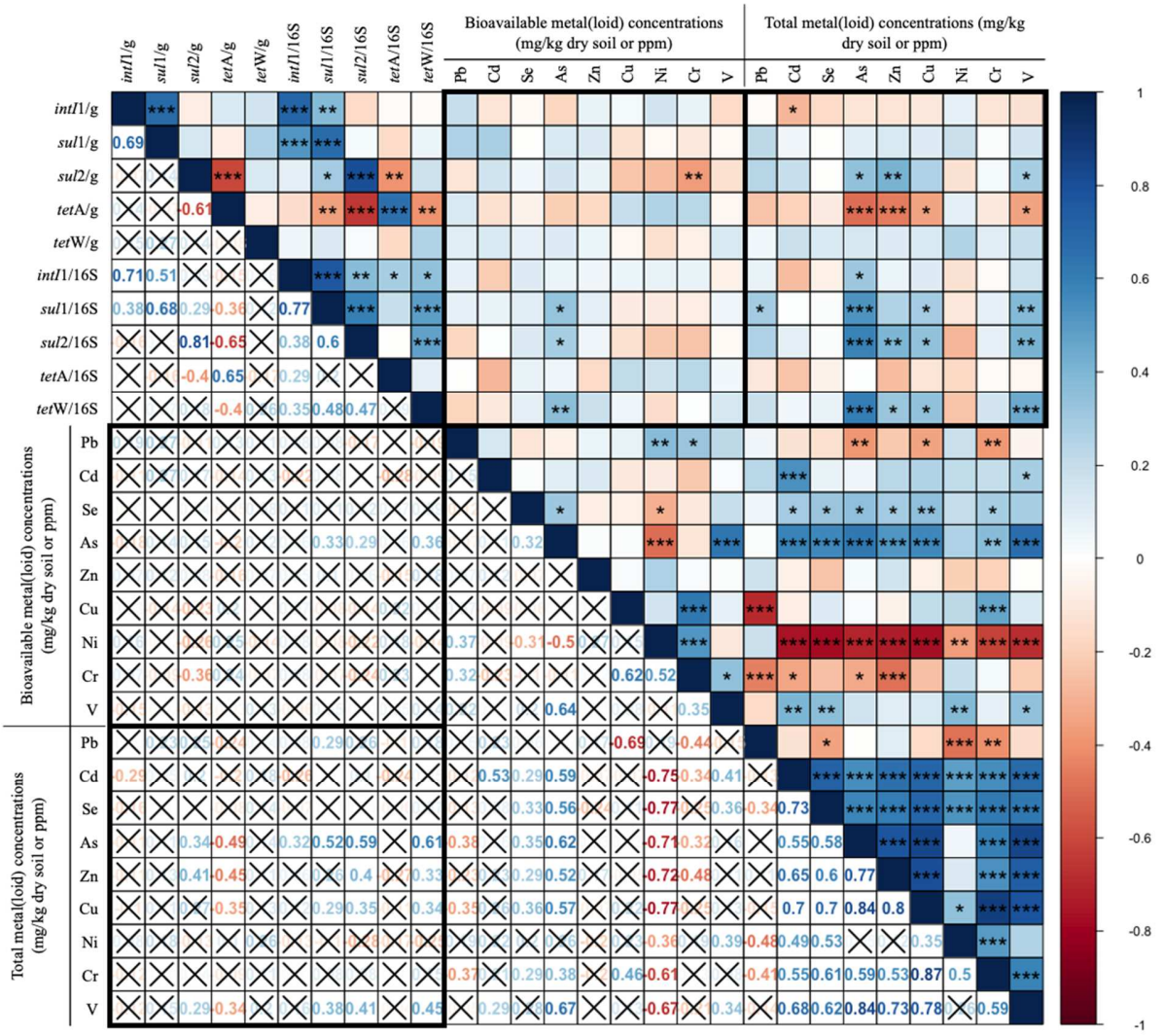

Figure 4. Pearson's correlation coefficients among log-transformed ARGs, a mobile genetic element (*intI*1), bioavailable metal(loid)s, and total metal(loid)s (positive = blue, negative = red, X = not significant). Correlations significant at $p < 0.001$, $p < 0.01$, and $p < 0.05$ are marked with ***, **, and *, respectively.

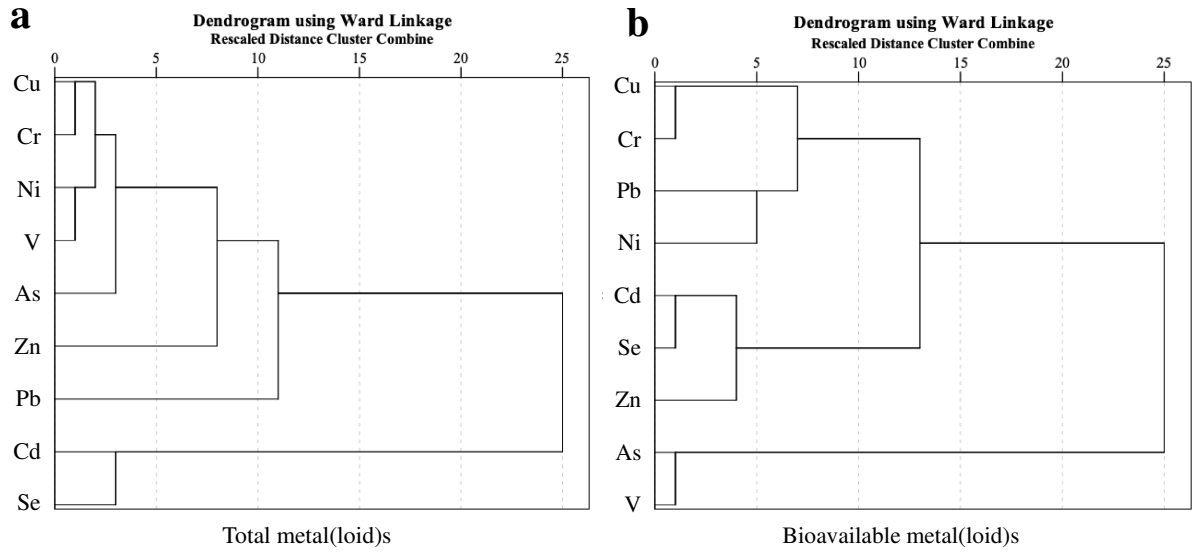

Figure 5. Dendrogram of hierarchical cluster analysis (HCA) for (a) total metal(loid)s and (b) bioavailable metal(loid)s quantified in soils across six GSI sites. The horizontal axis of the dendrogram represents the distance or dissimilarity between clusters. The vertical axis represents the objects and clusters. The distance between two clusters has been computed based on the length of the straight line drawn from one cluster to another.

356 *3.4. Soil characteristics of campus GSI*

357 GSI soil samples classified predominantly as sand, and to a lesser extent loamy sand or sandy
358 clay loam (Figure S5). Soil pH values ranged from slightly acidic (6.59) in the dry season to
359 strongly alkaline (9.05) in the post-wet season and exhibited some seasonality in MZ, VER, ACT,
360 and SAN (U.S. Department of Agriculture, 1998) (Figure S6). Soil moisture and SOM ranged
361 from 5.77% to 39.5% and from 1.22% to 15.5%, respectively (Table S5) and were relatively stable
362 across three time points (Figure S6).

363 Based on absolute abundances (normalized to grams of soil), many genes were significantly
364 and positively correlated with GSI soil characteristics (clay content, SOM, soil moisture, and total
365 C), including *intI*1 (clay: $r = 0.44$, adjusted $p < 0.001$; SOM: $r = 0.38$, adjusted $p < 0.01$; total C:
366 $r = 0.36$, adjusted $p < 0.01$) and *tet*A (clay: $r = 0.43$, adjusted $p < 0.001$; SOM: $r = 0.45$, adjusted
367 $p < 0.001$; total C: $r = 0.30$, adjusted $p < 0.05$) (Figure S7). Absolute gene abundances of *sul*1 were
368 positively correlated with clay content ($r = 0.32$, adjusted $p < 0.05$), SOM ($r = 0.29$, adjusted $p <$
369 0.05), PO_4 ($r = 0.39$, adjusted $p < 0.01$). Significant and negative correlations were also evident
370 between *sul*1/g and silt, *sul*2/g and silt, *sul*2/g and clay, and *tet*A/g and sand.

371 While most significant correlations between absolute gene abundances and soil
372 characteristics are positive, most significant correlations between relative gene abundances and
373 soil characteristics are negative. Relative gene abundances of both *sul*2 and *tet*W were significantly
374 negatively correlated with silt content (*sul*2: $r = -0.44$, adjusted $p < 0.001$; *tet*W: $r = -0.37$, adjusted
375 $p < 0.01$), clay content (*sul*2: $r = -0.41$, adjusted $p < 0.01$; *tet*W: $r = -0.31$, adjusted $p < 0.05$), SOM
376 (*sul*2: $r = -0.57$, adjusted $p < 0.001$; *tet*W: $r = -0.57$, adjusted $p < 0.001$), total C (*sul*2: $r = -0.47$,
377 adjusted $p < 0.001$; *tet*W: $r = -0.53$, adjusted $p < 0.001$), and NO_3-N (*sul*2: $r = -0.28$, adjusted $p <$
378 0.05; *tet*W: $r = -0.29$, adjusted $p < 0.05$). Relative gene abundances of *sul*1 were also significantly

negatively correlated with silt content (r = -0.57, adjusted $p < 0.001$) and SOM (r = -0.33, adjusted $p < 0.05$). Significant positive correlations between relative gene abundances and some soil characteristics were also evident, including, sand content and *sul*1/16S, sand content and *sul*2/16S, sand content and *tet*W/16S, pH and *intI*1/16S, and PO_4 and *intI*1/16S.

Significant correlations were also found between bioavailable metal(loid) concentrations and soil characteristics in collected GSI samples (Figure S8). Levels of CEC, Total C, Total N, and PO_4 were significantly negatively correlated with bioavailable concentrations of As (r = -0.30 to -0.38, adjusted $p < 0.05$) and Cu (r = -0.37 to -0.58, adjusted $p < 0.01$). In contrast, levels of CEC, Total C, Total N, and PO_4 were significantly positively correlated with bioavailable concentrations of Ni (r = 0.34 to 0.76, adjusted $p < 0.01$). In addition, bulk densities of GSI were significantly with bioavailable concentrations of Se (r = -0.31, adjusted $p < 0.05$), As (r = -0.48, adjusted $p < 0.001$), Cu (r = 0.44, adjusted $p < 0.001$), Ni (r = 0.56, adjusted $p < 0.001$), Cr (r = 0.31, adjusted $p < 0.05$), and V (r = –0.42, adjusted $p < 0.001$).

3.5. The influence of soil characteristics and metal(loid)s on AR

MLS was performed to determine the soil characteristics and metal(loid) concentrations most predictive of ARG and *intI*1 abundances in GSI. We used stepwise regression analysis to generate regression equations for both absolute and relative gene abundances (Table 2). From the resulting models we can infer that: (1) gene abundance in GSI soils is correlated with various subsets of soil properties and total metal(loid)s, but not with bioavailable metal(loid)s; (2) MLS models for relative gene abundances are all positively correlated with total As; and (3) with the exception *intI*1/g, all models of absolute gene abundances are correlated with soil texture. Most of the MLS models explain about 50% of the variance in absolute and relative gene abundances. The exception is the MLS models for *tet*A/g and *sul*2/16S, which explained 13% and 29% of the variance in gene abundances, respectively.

The scatter plots between the observed and the predicted values of gene abundances were used to verify the MLS results (Figure 6). Several significant relationships were found in *intI*1/g ($r = 0.65$, adjusted $p < 0.001$), *sul*1/g ($r = 0.40$, adjusted $p < 0.01$), *sul*2/g ($r = 0.74$, adjusted $p < 0.001$), *intI*1/16S ($r = 0.41$, adjusted $p < 0.001$), *tet*A/16S ($r = 0.47$, adjusted $p < 0.001$), and *sul*2/16S ($r = 0.63$, adjusted $p < 0.001$). Overall, MLS models provided significant improvement for estimating most relative and absolute abundances of ARGs and *intI*1 genes in GSI soils.

Table 2. Summary of multiple linear regression with a linear combination of bioavailable and total metal(loid) concentrations and soil characteristics. A stepwise method was adopted. All variables were log-transformed to ensure better normal distribution prior to MLS analysis.

Element	Equation	R^2	R^2_{adj}	p-value
*intI*1/g	$Log_{10}(intI1/g) = 1.187 + 0.979\ Log_{10}(PO_4\text{-}P) + 1.321\ Log_{10}(Moisture) + 0.440\ Log_{10}(Tot\ Cr)$	0.623	0.597	0.004
*sul*1/g	$Log_{10}(sul1/g) = 3.346 + 0.301\ Log_{10}(PO_4\text{-}P) + 0.257\ Log_{10}(Tot\ Cu) - 1.253\ Log_{10}(Silt) + 1.656\ Log_{10}(Clay) + 0.457\ Log_{10}(NH_4\text{-}N)$	0.613	0.567	0.01
*sul*2/g	$Log_{10}(sul2/g) = 35.584 - 0.130\ Log_{10}(Tot\ Zn) - 14.576\ Log_{10}(Sand) - 2.546\ Log_{10}(Silt) - 1.943\ Log_{10}(Clay)$	0.580	0.541	0.043
*tet*A /g	$Log_{10}(tetA/g) = 2.981 + 0.450\ Log_{10}(Clay)$	0.148	0.129	0.007
*tet*W /g	$Log_{10}(tetW/g) = -21.849 + 12.037\ Log_{10}(Sand) + 0.104\ Log_{10}(Tot\ Zn) + 1.872\ Log_{10}(CEC) + 1.656\ Log_{10}(Silt)$	0.548	0.506	0.012
*intI*1/16S	$Log_{10}(intI1/16S) = -21.6565 + 1.182\ Log_{10}(Moisture) + 0.922\ Log_{10}(Tot\ As) + 2.463\ Log_{10}(Clay) - 0.272\ Log_{10}(Total\ Cd) + 5.589\ Log_{10}(Sand)$	0.744	0.707	0.046
*sul*1/16S	$Log_{10}(sul1/16S) = -22.372 + 0.820\ Log_{10}(Tot\ As) + 3.833\ Log_{10}(Clay) + 8.663\ Log_{10}(Sand) - 0.132\ Log_{10}(Tot\ Cd)$	0.775	0.749	0.031
*sul*2/16S	$Log_{10}(sul2/16S) = -6.556 - 0.266\ Log_{10}(Tot\ Zn) + 0.753\ Log_{10}(Tot\ As) + 1.047\ Log_{10}(Moisture)$	0.335	0.289	0.027
*tet*A/16S	$Log_{10}(tetA/16S) = -7.737 - 0.919\ Log_{10}(Tot\ N) + 0.377\ Log_{10}(Tot\ As) + 1.186\ Log_{10}(Clay)$	0.657	0.633	0.002
*tet*W/16S	$Log_{10}(tetW/16S) = -13.554 + 4.526\ Log_{10}(Sand) + 1.145\ Log_{10}(Tot\ As) - 0.254\ Log_{10}(Tot\ Se) + 0.606\ Log_{10}(NH_4\text{-}N)$	0.696	0.668	0.024

Abbreviation: R^2, coefficient of determination; R^2_{adj}, adjusted coefficient of determination.

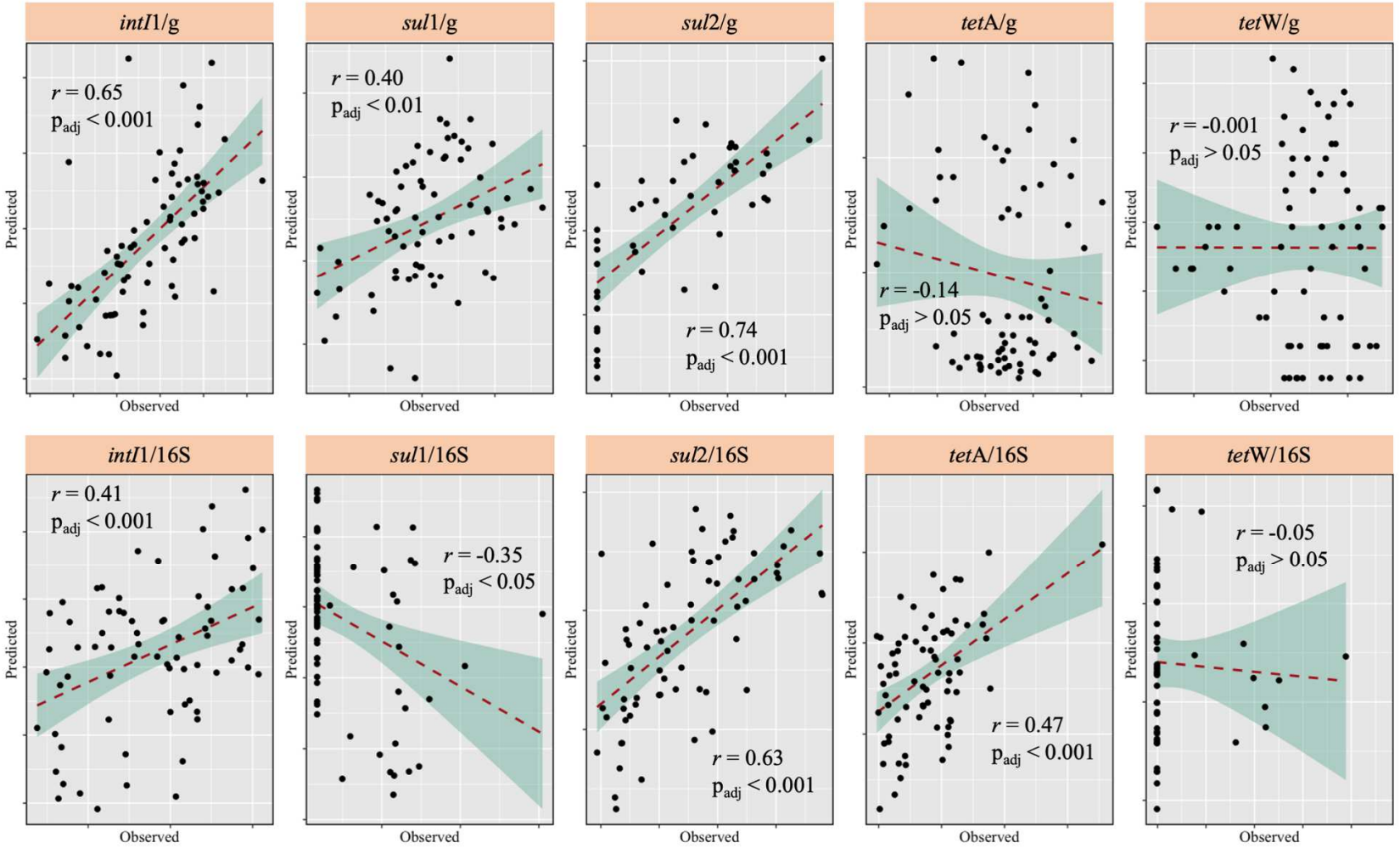

Figure 6. Pearson coefficients (*r*) between observed and predicted values of absolute and relative abundances of *sul*1, *sul*2, *tet*A, *tet*W, and *intI*1 genes based on multiple linear regression (MLS) models in GSI soils across three UC campuses (N = 72). Abbreviation: p_{adj}, Adjusted p value.

4. Discussion

4.1. Prevalence of ARGs in GSI soils

ARGs were frequently detected in GSI soil samples analyzed here. To place these results in context, we compared the relative *sul*1 and *intI*1 gene abundances measured in GSI soil samples to soils previously measured in wastewater treatment plant biosolids (Hung, 2020), Los Angeles park soils (Echeverria-Palencia et al., 2017), commercially available manure fertilizers, and native soils from nearby hiking trails (Cira et al., 2021) (Figure 7). Methods for sample collection, DNA extraction, and gene quantification were the same as described previously. These comparisons indicate (Figure 7): (1) relative gene abundances of *sul*1 and *intI*1 in GSI soils are higher in GSI soils compared to native soils collected from the Santa Monica Mountains near Los Angeles (Cira et al., 2021); (2) relative gene abundances of *sul*1 are lower in GSI soils compared to biosolids (Hung, 2020), commercially available manure fertilizers (Cira et al., 2021), and Los Angeles park soils (Echeverria-Palencia et al., 2017); and (3) relative gene abundances of *intI*1 in GSI soil also exhibit a similar pattern to relative gene abundances of *sul*1 (excluding San Diego park soils for which *intI*1 gene abundance measurements were not available) (Figure 7).

GSI management may play a critical role in soil ARG abundances. Soil amendments and reclaimed water, both of which are reservoirs for ARGs (Cira et al., 2021; Fahrenfeld et al., 2013; Mao et al., 2014), are frequently used for fertilizing and irrigating GSI (Rottle, 2018, 2013). In the present study, MZ, SM, CUL, and SAN were irrigated with reclaimed water while VER and ACT were irrigated with potable water (Table 1). Among all GSI elements included in our study, MZ was the only site that did not receive soil amendments; interestingly, this GSI element also had relatively low relative ARG abundances (Figure 2). On the other hand, of all GSI soils we sampled, relative *sul*1, *sul*2, *tet*W, and *intI*1 gene abundances were the highest at ACT. This particular site

444 is notable in that it was the only GSI element that we sampled that was irrigated with condensation
445 drainage from building air conditioners. The composition of GSI vegetation, site ages, total areas,
446 and their respective impervious drainage areas are also likely to affect the ARG levels in GSI soils.
447 (Zhou et al., 2021).
448

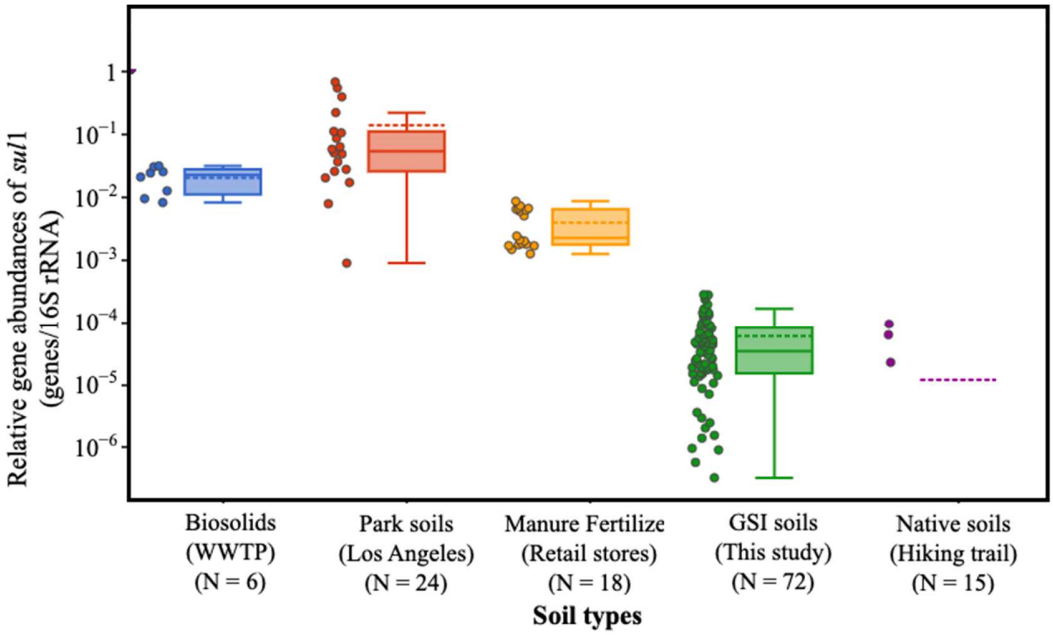

449

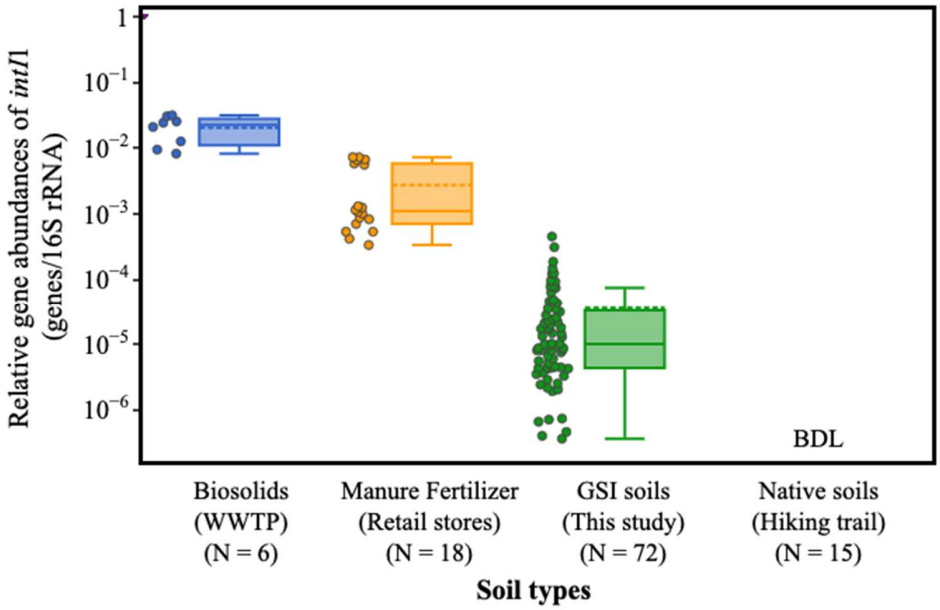

450

451 Figure 7. Relative gene abundances of *sul*1 (top) and *intI*1 (bottom) among soils of various
452 location types. Citation for studies sourced for the comparison data are within the Discussion.
453 The top and bottom boxes represent the 25th percentile and the 75th percentile. The whiskers
454 exclude outliers and extend 1.5 times the interquartile range from both edges of the box. Data
455 points were also shown next to their corresponding box plots. Abbreviation: BDL: Below
456 Detection Limit.

4.2. Metal(loid)s in GSI

Metal(loid)s are often present at high concentrations in stormwater runoff (Li et al., 2012), and consequently can accumulate in GSI soils (Chen et al., 2005). Relatively little research has been devoted to investigating seasonal variations in metal(loid)s and their co-selective effects on AR in urban GSI. Relatively high total concentrations of As, Cr, Cu, Ni, Se, V, and Zn during the rainy season (February/March) (Figure 3 and Figure S3) observed in this study are generally consistent with previously published findings that, with the exception of Pb, wet weather events in Southern California tend to carry higher metal(loid) concentrations (Lee et al., 2004). A possible explanation for the different seasonal pattern of Pb is that Pb compounds are mainly particulate-bound while other metal(loid)s are mainly in dissolved forms in stormwater runoff (Sansalone and Buchberger, 1997). Importantly, in our study both spatial and temporal variability in metal(loid) concentrations are strongly associated with variations in absolute and relative gene abundances (see MLS models in Table 2), consistent with our metal(loid) co-selection hypothesis.

Indeed, many recent studies have shown significantly positive correlations between ARGs and total metal(loid)s in soils collected from diverse environments, including (Table 3): (1) the relative gene abundance of *tet*W was correlated with total Cu concentrations in archived soils from the 1940s to the 1970s (Knapp et al., 2011); (2) relative gene abundances of *sul*1 and *sul*2 were correlated with total Cu concentrations in Chinese agricultural soils and manure (Cui et al., 2016; Zhang et al., 2018). However, relative gene abundances of *tet*W demonstrated no significant correlations with total concentrations of Zn, As, Cu in animal manure and agricultural soils. Absolute gene abundances of *tet*A were negatively correlated with the several total metal(loid) concentrations. Such variations in correlation results may reflect that relationships vary depending on whether sampled environments are moderately versus highly polluted. Tetracycline resistance genes were more prevalent and frequently detected in animal manure and agricultural soils than in GSI soils (Ji et al., 2012). Although correlations do not necessarily represent causation, taken together these findings suggest that trace levels of metal(loid)s exert selective pressure on the emergence of ARGs across a range of natural and urban environments.

Unlike total metal(loid)s, limited studies have reported the correlations between bioavailable metal(loid)s (Table 3). A similar study indicated that bioavailable As was correlated with relative gene abundances of *sul*1 and *tet*W within chicken manure, but their correlation coefficients were higher than our correlation results (Cui et al., 2016). Bioavailable metal(loid)s, rather than total metal(loid)s, may play a more important role for microbial communities since they may be able to penetrate cytoplasmic membranes and trigger metal resistance (Roosa et al., 2014). Bioavailability of metal(loid)s depend on multiple factors, such as the origin and nature of metal(loid)s, soil physico-chemical processes, and soil microbial taxa (Olaniran et al., 2013). In the present study,

492 the bioavailable fraction of metal(loid)s in GSI appeared to be low, potentially contributing to
493 limited co-selective effects on ARGs.

494 Correlation results also suggested that metal(loid)s are more likely to influence ARGs as
495 groups than as individual metal(loid)s in complex soil environments, since many of them are co-
496 occurring. In this study, many strong and positive correlations were found among all total
497 metal(loid)s except for Pb–Se, Pb–Ni, and Pb–Cr, all of which showed negative relationships (Pb–
498 Se: r = -0.34, adjusted $p < 0.05$; Pb–Ni: r = -0.48, adjusted $p < 0.001$; Pb–Cr: r = -0.41, adjusted p
499 < 0.01) (Figure 4). Further, the HCA results (Figure 5) suggested that metal(oid)s including Zn,
500 Cu, Cr, and Ni serve as micronutrients in various physiological functions of biological cells.
501 Further, metal(loid)s are not equally toxic to bacteria. The three outliers, Pb, Se and Cd clustered
502 in rather far away at much higher distance (Figure 5), supporting previous hypothesis about their
503 significantly reduced relevance as microelements (Seiler and Berendonk, 2012). Overall, as per
504 this study, soil environments with lower metal(loid) concentrations, for example, GSI, may exhibit
505 co-occurring patterns of total metal(loid) loading that can simultaneously trigger co-selection of
506 AR.

507 To assess the risk of metal(loid) co-selection on AR, the concept of minimum co-selective
508 concentrations (MCC) was previously adopted and evaluated for many environmental
509 compartments by Seiler and Berendonk (2012) and Arya et al. (2021). More specifically, minimum
510 metal(loid)s concentrations associated with increased ARG abundances were defined as MCC.
511 Since metal(loid) concentrations varied greatly in the environments, metal(loid)s exceeding their
512 MCCs in their respective environments may be co-selective for ARGs. Currently, there are only a
513 few studies reporting MCC datasets in soil environments (Arya et al., 2021; Seiler and Berendonk,
514 2012), with no MCC datasets considering GSI settings studied here. Therefore, the assessment of

515 metal(loid) co-selective effects on AR in GSI soils is limited. Several minimum metal(loid)
516 measurements (Cu, Pb, and Zn) within GSI soils herein were lower than reported MCCs (Cu: 11.5
517 mg/kg and Zn: 42.5 mg/kg) (Seiler and Berendonk, 2012) or (Cu: 1.6 mg/L, Pb: 21.5 mg/L, and
518 Zn: 5.5 mg/L) (Arya et al., 2021) in other soil environments, yet they were still correlated with the
519 *sul*1/16S, *sul*2/16S, and *tet*W/16S , respectively. Other metal(loid)s, such as Se, Ni, and Cr, within
520 the GSI soils herein were also lower compared to MCCs in other soil environments and may be
521 within the range of no co-selection effects. In sum, soil environments with relatively low
522 concentrations of metal(loid)s, particularly in GSI soils, are still likely to facilitate co-selection of
523 AR. Multiple effects of metal(loid)s may need to be considered given that inter-correlations
524 between metal(loid)s were high. For microbial risk assessment purposes as related to AR, GSI
525 soils data herein suggest that metal(loid) concentrations should also receive attention.

Table 3. Significant correlations between ARGs (and *intI*1 genes) and metal(loid)s in soils reported in previous studies (Cui et al., 2016; He et al., 2014; Ji et al., 2012; Knapp et al., 2017, 2011; Zhang et al., 2018). Bordered genes indicate correlations are overlapping with the present study. Negative signs indicate negative correlations.

Element	List of ARGs significantly correlated with the element			
	Absolute gene abundances (per gram)		Relative gene abundances (per 16S rRNA)	
	Ct.	Type	Ct.	Type
Total metal(loid)s				
Aluminum (Al)	6	*bla*$_{TEM}$, *bla*$_{OXA}$, *tet*M, *tet*W, *sul*2, *sul*3	1	*bla*$_{TEM}$
Arsenic (As)	1	*bla*$_{SHV}$	11	*bla*$_{SHV}$, *tet*BP, *fex*A, *fex*B, *cfr*, *sul*1, *intI*1, *tet*H, *tet*O, *tetQ*, *tet*W
Cadmium (Cd)	1	*bla*$_{OXA}$	0	
Chromium (Cr)	1	*tet*T	5	*bla*$_{CTX}$, *bla*$_{OXA}$, *tet*M, *tet*O, *tet*S
Cobalt (Co)	0		1	*tet*M
Copper (Cu)	5	*bla*$_{TEM}$, *bla*$_{OXA}$, *tet*M, *tet*T, *dfr*A12(-)	20	*tet*M, *tet*W, *bla*$_{OXA}$, *erm*B, *erm*F, *sul*A, *sul*3, *tet*A, *tet*B, *tet*Q, *tet*X, *sul*1, *sul*2, *cfr*, *fex*A, *fex*B, *cfr*, *intI*1, *tet*O, *tet*S
Mercury (Hg)	1	*tet*2	2	*tet*2 (-), *sul*A
Manganese (Mn)	8	*bla*$_{TEM}$, *bla*$_{CTX}$, *bla*$_{OXA}$, *tet*4, *tet*M, *tet*W, *sul*1, *sul*2	9	*bla*$_{TEM}$, *tet*2 (-), *fex*A, *fex*B, *cfr*, *sul*1, *tet*O, *tet*S, *tet*W
Nickel (Ni)	3	*bla*$_{TEM}$, *bla*$_{OXA}$, *tet*T	3	*bla*$_{SHV}$, *tet*2 (-), *tet*W
Lead (Pb)	4	*bla*$_{OXA}$, *tet*2 (-), *dfr*A12 (-), *erm*ATR	3	*bla*$_{TEM}$, *bla*$_{OXA}$, *tet*2 (-)
Selenium (Se)	0		1	*tet*3
Strontium (Sr)	0		10	*fex*A, *fex*B, *cfr*, *sul*1, *intI*1, *tet*O, *tetQ*, *tetS*, *tet*W, *tet*T
Uranium (U)	2	*bla*$_{TEM}$, *bla*$_{CTX}$	3	*bla*$_{TEM}$, *bla*$_{CTX}$, *bla*$_{SHV}$
Vanadium (V)	8	*bla*$_{TEM}$, *bla*$_{CTX}$, *bla*$_{OXA}$, *tet*2 (-), *tet*4, *tet*W, *sul*1, *sul*2	1	*tet*2 (-)
Zinc (Zn)	4	*bla*$_{TEM}$, *bla*$_{OXA}$, *tet*T, *tet*W	11	*sul*A, *sul*3, *tet*L, *tet*W, *tet*Q, *sul*1, *sul*2, *fex*A, *fex*B, *cfr*, *intI*1
Bioavailable metal(loid)s				
Arsenic (As)	0		8	*tet*A, *tet*L, *tet*M, *tet*W, *tet*Q, *sul*1, *cfr*, *fex*A
Copper (Cu)	0		2	*tet*A, *flo*R
Iron (Fe)	0		1	*tet*M
Zinc (Zn)	0		10	*intI*1, *tet*B, *tet*M, *tet*Q, *tet*X, *sul*1, *sul*2, *cfr*, *cml*A, *flo*R

Abbreviation: Ct: Count.

4.3. Soil characteristics of campus GSI in Southern California

In the present study, correlation analysis indicated many significant correlations among ARGs, metal(loid)s, and soil characteristics, such as soil texture and amount of nutrients, which were in accordance with previous studies. Previous investigation in Antarctic soils indicated soil texture influenced the relative abundance of ARGs (Wang et al., 2016). Moreover, two studies conducted in surface sediment near mariculture in Donying and in the Dongjiang River basin in China indicated that nutrients explained certain variation in ARGs, with some ARGs showing association with total organic carbon and total N (Su et al., 2014; Zhao et al., 2017). Agricultural soils frequently irrigated with wastewater in Mezquital Valley, Mexico, over a period of 100 years also showed significant correlations between ARG abundances and phosphorus concentrations, but no significant correlations between soil pH and ARGs (Jechalke et al., 2015).

Most significant correlations between absolute ARG abundances and soil characteristics were positive. One possibility is that bioavailable metal(loid)s in soils were mainly ~~mediated~~ affected by soil characteristics, such as the clay content and SOM (Violante et al., 2010). Similarly, soil characteristics herein appeared to affect bioavailable metal(loid)s (Figure S8). The increased concentrations of bioavailable metal(loid)s are likely to increase metal(loid) selection pressure on ARGs. Meanwhile, this work also suggested the clay content, SOM, total C, and total N were highly linked with 16S rRNA genes. Due to the co-linearity of 16S rRNA genes, most correlation results herein between relative ARG abundances and soil characteristics became negative. In sum, our results provided evidence that ARG abundances are related to soil characteristics in GSI. In addition to metal(loid)s, factors such as soil physico-chemical properties were shown to indirectly drive the selection of AR.

552 *4.4. Multiple linear regression models*

553 To comprehensively examine the multiple effects of soil characteristics, bioavailable
554 metal(loid)s, and total metal(loid)s on gene abundances in GSI, MLS results were performed and
555 indicated many significant relationships. Our MLS model in predicting *sul*2/16S supported
556 previous MLS model results in residential soils in Western Australia (Knapp et al., 2017). However,
557 our MLS models had no significant improvement of predicting both relative and absolute gene
558 abundances of and *sul*1 and *tet*W, suggesting other factors impacting gene abundances. In fact,
559 relative abundances of the *intI*1 gene have been suggested as a good indicator of anthropogenic
560 pollution and are commonly linked to genes conferring resistance to antibiotics and metal(loid)s
561 (Gillings et al., 2015). In the present study, the relative gene abundances of *intI*1 were significantly
562 correlated with relative gene abundances of *sul*1 ($r = 0.77$, adjusted $p < 0.001$) and *tet*W ($r = 0.35$,
563 adjusted $p < 0.05$). These findings suggested that the propagation of *sul*1 and *tet*W may be
564 facilitated by HGT of class 1 integron-integrase genes (*intI*1) in GSI soils. Overall, compared to
565 previous correlation results, inclusion of both physiological soil and metal(loid) factors in most
566 MLS models caused improvement in the relationship with ARG abundances.

567

568 *4.5. Limitations*

569 The association between metal(loid)s and AR has been widely identified in environmental
570 compartments for decades, including agricultural soils, wastewater, and animal manure. However,
571 prevalence of ARGs and their association with metal(loid)s in GSI soils is largely unknown. Our
572 results indicate the co-occurrence of ARGs, metal(loid)s, and soil characteristics in GSI soils over
573 three time periods. Urban stormwater is known to contain metal(loid)s (Li et al., 2012) that can
574 trigger co-selection on AR (Stepanauskas et al., 2006) and accumulate in the stormwater bio-
575 retention media (Al-Ameri et al., 2018). More efforts focusing on concentrations of metal(loid)s,
576 antibiotics, microbial communities, and ARGs in stormwater runoff entering GSI will elucidate
577 whether metal(loid) co-selection effects on ARGs exist before entering GSI media. Furthermore,
578 the transiently saturated nature of GSI (during storms) and associated shifts in sediment redox
579 conditions, which can influence metal(loid)s speciation, may facilitate the proliferation of ARGs
580 through co-selection. Exploring how hydrological and physico-chemical in these highly dynamic
581 systems influence, either positively or negatively, metal(loid) co-selection on AR is an interesting
582 topic for future research.

583

5. Conclusion

Despite the restricted use of some key antibiotics, other factors still contribute to the spread of AR and need to be understood. Metal(loid)s have been shown to exert selective pressure on environmental microbes. While urban GSI is known for metal(loid) and microorganism removal, studies addressing the relationship between metal(loid)s and microorganisms that accumulate in GSI media have yet to be directly investigated. Urban GSI soils are likely to be another potential environment that promotes the spread of ARGs via metal(loid) co-selection and poses a critical global health threat. Our results indicated that *intI*1 and ARGs were associated with many total metal(loid)s but limited bioavailable metal(loid)s. Based on the metal(loid) concentrations that correlated with genes, we found lower concentrations of metal(loid)s that co-select for ARGs in GSI compared to other soil environments. In addition to metal(loid)s, soil characteristics, such as soil texture and nutrients were shown to contribute to the prevalence of AR. MLS models combining aforementioned factors improved the relationships between observed and predicted gene abundances. To our knowledge, this work proposed the first multiple linear regression models with the inclusion of soil characteristics, total, and bioavailable metal(loid)s for ARGs in soil environments. Strong and significant regression coefficients were identified, implying additional stressors may govern the selection of AR. The results from this study could inform the design and management of urban GSI elements in mitigating the spread of AR based on soil features—such as co-occurring metal(loid)s, nutrients, soil characteristics, and their spatial-temporal patterns.

6. Acknowledgements

Funding was provided by the University of California Office of the President, Multicampus Research Programs and Initiatives, Grant ID MRP-17-455083. This material is based upon research performed in a collaborative laboratory space renovated by the National Science Foundation [grant number 0963183], which is an award funded under the American Recovery and Reinvestment Act of 2009 (ARRA).

611 **7. References**

612 Ahn, J.H., Grant, S.B., Surbeck, C.Q., Digiacomo, P.M., Nezlin, N.P., Jiang, S., 2005. Coastal
613 water quality impact of stormwater runoff from an urban watershed in Southern California.
614 Environ. Sci. Technol. 39, 5940–5953. https://doi.org/10.1021/es0501464
615 Al-Ameri, M., Hatt, B., Le Coustumer, S., Fletcher, T., Payne, E., Deletic, A., 2018.
616 Accumulation of heavy metals in stormwater bioretention media: A field study of temporal
617 and spatial variation. J. Hydrol. 567, 721–731. https://doi.org/10.1016/j.jhydrol.2018.03.027
618 Ambrose, R.F., Winfrey, B.K., 2015. Comparison of stormwater biofiltration systems in
619 Southeast Australia and Southern California. Wiley Interdiscip. Rev. Water 2, 131–146.
620 https://doi.org/10.1002/wat2.1064
621 Arya, S., Williams, A., Reina, S.V., Knapp, C.W., Kreft, J.U., Hobman, J.L., Stekel, D.J., 2021.
622 Towards a general model for predicting minimal metal concentrations co-selecting for
623 antibiotic resistance plasmids. Environ. Pollut. 275, 116602.
624 https://doi.org/10.1016/j.envpol.2021.116602
625 Askarizadeh, A., Rippy, M.A., Fletcher, T.D., Feldman, D.L., Peng, J., Bowler, P., Mehring,
626 A.S., Winfrey, B.K., Vrugt, J.A., Aghakouchak, A., Jiang, S.C., Sanders, B.F., Levin, L.A.,
627 Taylor, S., Grant, S.B., 2015. From Rain Tanks to Catchments: Use of Low-Impact
628 Development To Address Hydrologic Symptoms of the Urban Stream Syndrome. Environ.
629 Sci. Technol. 49, 11264–11280. https://doi.org/10.1021/acs.est.5b01635
630 Association of Official Analytical Chemists (AOAC), 1997. Official Method 972.43,
631 Microchemical determination of carbon, hydrogen, and nitrogen, in: Official Methods of
632 Analysis of AOAC International. AOAC International, Arlington, VA, pp. 5 – 6.
633 Baker-Austin, C., Wright, M.S., Stepanauskas, R., McArthur, J. V., 2006. Co-selection of
634 antibiotic and metal resistance. Trends Microbiol. 14, 176–182.
635 https://doi.org/10.1016/j.tim.2006.02.006
636 Benjamini, Y., Hochberg, Y., 1995. Controlling the False Discovery Rate : A Practical and
637 Powerful Approach to Multiple Testing Yoav Benjamini ; Yosef Hochberg Journal of the
638 Royal Statistical Society . Series B (Methodological) , Vol . 57 , No . 1 . (1995), pp . 57,
639 289–300.
640 Blecken, G.T., Zinger, Y., Deletić, A., Fletcher, T.D., Viklander, M., 2009. Influence of
641 intermittent wetting and drying conditions on heavy metal removal by stormwater biofilters.
642 Water Res. 43, 4590–4598. https://doi.org/10.1016/j.watres.2009.07.008

643 Bradford, G.R., Change, A.C., Page, A.L., Bakhtar, D., Frampton, J.A., Wright, H., 1996.
644 Background Concentrations of Trace and Major Elements in California Soils.
645 Bustin, S.A., Benes, V., Garson, J.A., Hellemans, J., Huggett, J., Kubista, M., Mueller, R.,
646 Nolan, T., Pfaffl, M.W., Shipley, G.L., Vandesompele, J., Wittwer, C.T., 2009. The MIQE
647 guidelines: Minimum information for publication of quantitative real-time PCR
648 experiments. Clin. Chem. 55, 611–622. https://doi.org/10.1373/clinchem.2008.112797
649 Cal DTSC, 2020. Human Health Risk Assessment (HHRA) Note Number 7, DTSC-modified
650 Screening Levels (DTSC-SLs).
651 Chee-Sanford, J.C., Mackie, R.I., Koike, S., Krapac, I.G., Lin, Y.-F., Yannarell, A.C., Maxwell,
652 S., Aminov, R.I., 2009. Fate and Transport of Antibiotic Residues and Antibiotic Resistance
653 Genes following Land Application of Manure Waste. J. Environ. Qual. 38, 1086–1108.
654 https://doi.org/10.2134/jeq2008.0128
655 Cira, M., Echverria-Palencia, C.M., Callejas, I., Jimenez, K., Herrera, R., Hung, W., Colima, N.,
656 Schmidt, A., Jay, J., 2021. Commercially available garden products as important sources of
657 antibiotic resistance genes—A survey. Environ. Sci. Pollut. Res.
658 https://doi.org/https://doi.org/10.1007/s11356-021-13333-7
659 Cui, E., Wu, Y., Zuo, Y., Chen, H., 2016. Effect of different biochars on antibiotic resistance
660 genes and bacterial community during chicken manure composting. Bioresour. Technol.
661 203, 11–17. https://doi.org/10.1016/j.biortech.2015.12.030
662 Cycoń, M., Mrozik, A., Piotrowska-Seget, Z., 2019. Antibiotics in the soil environment—
663 degradation and their impact on microbial activity and diversity. Front. Microbiol. 10.
664 https://doi.org/10.3389/fmicb.2019.00338
665 Czekalski, N., Sigdel, R., Birtel, J., Matthews, B., Bürgmann, H., 2015. Does human activity
666 impact the natural antibiotic resistance background? Abundance of antibiotic resistance
667 genes in 21 Swiss lakes. Environ. Int. 81, 45–55.
668 https://doi.org/10.1016/j.envint.2015.04.005
669 Di Cesare, A., Eckert, E.M., Corno, G., 2016. Co-selection of antibiotic and heavy metal
670 resistance in freshwater bacteria. J. Limnol. 75, 59–66.
671 https://doi.org/10.4081/jlimnol.2016.1198
672 Dorsey, J.H., Carmona-Galindo, V.D., Leary, C., Huh, J., Valdez, J., 2013. An assessment of
673 fecal indicator and other bacteria from an urbanized coastal lagoon in the City of Los
674 Angeles, California, USA. Environ. Monit. Assess. 185, 2647–2669.

https://doi.org/10.1007/s10661-012-2737-3
Echeverria-Palencia, C.M., Thulsiraj, V., Tran, N., Ericksen, C.A., Melendez, I., Sanchez, M.G., Walpert, D., Yuan, T., Ficara, E., Senthilkumar, N., Sun, F., Li, R., Hernandez-cira, M., Gamboa, D., Haro, H., Paulson, S.E., Zhu, Y., Jay, J.A., 2017. Disparate Antibiotic Resistance Gene Quantities Revealed across 4 Major Cities in California: A Survey in Drinking Water, Air, and Soil at 24 Public Parks. ACS Omega 2, 2255–2263. https://doi.org/10.1021/acsomega.7b00118
Fahrenfeld, N., Ma, Y., O'Brien, M., Pruden, A., 2013. Reclaimed water as a reservoir of antibiotic resistance genes: Distribution system and irrigation implications. Front. Microbiol. 4, 1–10. https://doi.org/10.3389/fmicb.2013.00130
Gao, P., Munir, M., Xagoraraki, I., 2012. Correlation of tetracycline and sulfonamide antibiotics with corresponding resistance genes and resistant bacteria in a conventional municipal wastewater treatment plant. Sci. Total Environ. 421–422, 173–183. https://doi.org/10.1016/j.scitotenv.2012.01.061
Gardner, W.H., 1986. Water content, in: Klute, A. (Ed.), Methods of Soil Analysis, Part 1, Physical and Mineralogical Methods. American Society of Agronomy, Agronomy Monographs 9(1), Madison, WI, pp. 493–544.
Garner, E., Benitez, R., von Wagoner, E., Sawyer, R., Schaberg, E., Hession, W.C., Krometis, L.-A.H., Badgley, B.D., Pruden, A., 2017. Stormwater loadings of antibiotic resistance genes in an urban stream. water Res. 123, 144–152. https://doi.org/http://dx.doi.org/10.1016/j.watres.2017.06.046
Gillings, M.R., Gaze, W.H., Pruden, A., Smalla, K., Tiedje, J.M., Zhu, Y.G., 2015. Using the class 1 integron-integrase gene as a proxy for anthropogenic pollution. ISME J. 9, 1269–1279. https://doi.org/10.1038/ismej.2014.226
Graham, D.W., Olivares-Rieumont, S., Knapp, C.W., Lima, L., Werner, D., Bowen, E., 2011. Antibiotic resistance gene abundances associated with waste discharges to the Almendares river near Havana, Cuba. Environ. Sci. Technol. 45, 418–424. https://doi.org/10.1021/es102473z
Grant, S.B., Fletcher, T.D., Feldman, D., Saphores, J.D., Cook, P.L.M., Stewardson, M., Low, K., Burry, K., Hamilton, A.J., 2013. Adapting urban water systems to a changing climate: Lessons from the millennium drought in southeast Australia. Environ. Sci. Technol. 47, 10727–10734. https://doi.org/10.1021/es400618z

Grant, S.B., Saphores, J.D., Feldman, D.L., Hamilton, A.J., Fletcher, T.D., Cook, P.L.M., Stewardson, M., Sanders, B.F., Levin, L.A., Ambrose, R.F., Deletic, A., Brown, R., Jiang, S.C., Rosso, D., Cooper, W.J., Marusic, I., 2012. Taking the "waste" out of "wastewater" for human water security and ecosystem sustainability. Science (80-.). 337, 681–686. https://doi.org/10.1126/science.1216852

He, L.Y., Liu, Y.S., Su, H.C., Zhao, J.L., Liu, S.S., Chen, J., Liu, W.R., Ying, G.G., 2014. Dissemination of antibiotic resistance genes in representative broiler feedlots environments: Identification of indicator ARGs and correlations with environmental variables. Environ. Sci. Technol. 48, 13120–13129. https://doi.org/10.1021/es5041267

He, L.Y., Ying, G.G., Liu, Y.S., Su, H.C., Chen, J., Liu, S.S., Zhao, J.L., 2016. Discharge of swine wastes risks water quality and food safety: Antibiotics and antibiotic resistance genes from swine sources to the receiving environments. Environ. Int. 92–93, 210–219. https://doi.org/10.1016/j.envint.2016.03.023

Helsel, D.R., Gilloom, R.J., 1986. Estimation of distributional parameters for censored water quality data. Dev. Water Sci. 27, 137–157. https://doi.org/10.1016/S0167-5648(08)70789-5

Hu, H.W., Wang, J.T., Li, J., Shi, X.Z., Ma, Y.B., Chen, D., He, J.Z., 2017. Long-term nickel contamination increases the occurrence of antibiotic resistance genes in agricultural soils. Environ. Sci. Technol. 51, 790–800. https://doi.org/10.1021/acs.est.6b03383

Hung, W.-C., Hernandez-Cira, M., Jimenez, K., Elston, I., Jay, J.A., 2018. Preliminary assessment of lead concentrations in topsoil of 100 parks in Los Angeles, California. Appl. Geochemistry 99. https://doi.org/10.1016/j.apgeochem.2018.10.003

Hung, W., 2020. Prevalence, Fate, and Co-selection of Heavy Metals and Antibiotic Resistance Genes in Urban and Agricultural Soils. University of California, Los Angeles.

Isaac Najera, Chu-Ching Lin, Golenaz Adeli Kohbodi, and, Jay*, J.A., 2005. Effect of Chemical Speciation on Toxicity of Mercury to Escherichia coli Biofilms and Planktonic Cells. https://doi.org/10.1021/ES048549B

Jang, H.M., Lee, J., Choi, S., Shin, J., Kan, E., Kim, Y.M., 2018. Response of antibiotic and heavy metal resistance genes to two different temperature sequences in anaerobic digestion of waste activated sludge. Bioresour. Technol. 267, 303–310. https://doi.org/10.1016/j.biortech.2018.07.051

Jechalke, S., Broszat, M., Lang, F., Siebe, C., Smalla, K., Grohmann, E., 2015. Effects of 100 years wastewater irrigation on resistance genes, class 1 integrons and IncP-1 plasmids in

739 Mexican soil. Front. Microbiol. 6, 1–10. https://doi.org/10.3389/fmicb.2015.00163
740 Ji, X., Shen, Q., Liu, F., Ma, J., Xu, G., Wang, Y., Wu, M., 2012. Antibiotic resistance gene
741 abundances associated with antibiotics and heavy metals in animal manures and agricultural
742 soils adjacent to feedlots in Shanghai; China. J. Hazard. Mater. 235–236, 178–85.
743 https://doi.org/10.1016/j.jhazmat.2012.07.040
744 Karkman, A., Pärnänen, K., Larsson, D.G.J., 2019. Fecal pollution can explain antibiotic
745 resistance gene abundances in anthropogenically impacted environments. Nat. Commun.
746 10, 1–8. https://doi.org/10.1038/s41467-018-07992-3
747 Knapp, C.W., Callan, A.C., Aitken, B., Shearn, R., Koenders, A., Hinwood, A., 2017.
748 Relationship between antibiotic resistance genes and metals in residential soil samples from
749 Western Australia. Environ. Sci. Pollut. Res. 24, 2484–2494.
750 https://doi.org/10.1007/s11356-016-7997-y
751 Knapp, C.W., McCluskey, S.M., Singh, B.K., Campbell, C.D., Hudson, G., Graham, D.W.,
752 2011. Antibiotic resistance gene abundances correlate with metal and geochemical
753 conditions in archived Scottish soils. PLoS One 6, e27300.
754 https://doi.org/10.1371/journal.pone.0027300
755 Lee, H., Lau, S.L., Kayhanian, M., Stenstrom, M.K., 2004. Seasonal first flush phenomenon of
756 urban stormwater discharges. Water Res. 38, 4153–4163.
757 https://doi.org/10.1016/j.watres.2004.07.012
758 Li, W., Shen, Z., Tian, T., Liu, R., Qiu, J., 2012. Temporal variation of heavy metal pollution in
759 urban stormwater runoff. Front. Environ. Sci. Eng. China 6, 692–700.
760 https://doi.org/10.1007/s11783-012-0444-5
761 Manaia, C.M., Macedo, G., Fatta-Kassinos, D., Nunes, O.C., 2016. Antibiotic resistance in urban
762 aquatic environments: can it be controlled? Appl. Microbiol. Biotechnol. 100, 1543–1557.
763 https://doi.org/10.1007/s00253-015-7202-0
764 Mao, D., Luo, Y., Mathieu, J., Wang, Q., Feng, L., Mu, Q., Feng, C., Alvarez, P.J.J., 2014.
765 Persistence of extracellular DNA in river sediment facilitates antibiotic resistance gene
766 propagation. Environ. Sci. Technol. 48, 71–78. https://doi.org/10.1021/es404280v
767 Mao, D., Yu, S., Rysz, M., Luo, Y., Yang, F., Li, F., Hou, J., Mu, Q., Alvarez, P.J.J., 2015.
768 Prevalence and proliferation of antibiotic resistance genes in two municipal wastewater
769 treatment plants. Water Res. 85, 458–466. https://doi.org/10.1016/j.watres.2015.09.010
770 Martínez, J.L., 2008. Antibiotics and antibiotic resistance genes in natural environments. Science

771 (80-.). https://doi.org/10.1126/science.1159483
772 Mulvaney, R.L., 1996. Nitrogen – inorganic forms, in: Sparks, D.L. (Ed.), Methods of Soil
773 Analysis, Part 3 – Chemical Methods. SSSA Book Series No. 5. Soil Science Society of
774 America, Madison, WI, pp. 1129–1131.
775 National Oceanic and Atmospheric Administration, 2019. Monthly Precipitation Summary
776 Water Year 2019 [WWW Document]. URL
777 https://www.cnrfc.noaa.gov/monthly_precip_2018.php (accessed 12.1.21).
778 Nelson, D.W., Sommers, L.E., 1996. Total carbon, organic carbon, and organic matter, in:
779 Sparks, D.L. (Ed.), Methods of Soil Analysis, Part 3 – Chemical Methods. SSSA Book
780 Series No. 5. Soil Science Society of America, Madison, WI, pp. 1002–1005.
781 Olaniran, A.O., Balgobind, A., Pillay, B., 2013. Bioavailability of heavy metals in soil: Impact
782 on microbial biodegradation of organic compounds and possible improvement strategies.
783 Int. J. Mol. Sci. 14, 10197–10228. https://doi.org/10.3390/ijms140510197
784 Parker, E.A., Rippy, M.A., Mehring, A.S., Winfrey, B.K., Ambrose, R.F., Levin, L.A., Grant,
785 S.B., 2017. Predictive Power of Clean Bed Filtration Theory for Fecal Indicator Bacteria
786 Removal in Stormwater Biofilters. Environ. Sci. Technol. 51, 5703–5712.
787 https://doi.org/10.1021/acs.est.7b00752
788 Peng, J., Cao, Y., Rippy, M.A., Afrooz, A.R.M.N., Grant, S.B., 2016. Indicator and pathogen
789 removal by low impact development best management practices. Water (Switzerland) 8, 1–
790 24. https://doi.org/10.3390/w8120600
791 Pierce, G., Gmoser-Daskalakis, K., Rippy, M.A., Holden, P.A., Grant, S.B., Feldman, D.L.,
792 Ambrose, R.F., 2021. Environmental Attitudes and Knowledge: Do They Matter for
793 Support and Investment in Local Stormwater Infrastructure? Soc. Nat. Resour.
794 https://doi.org/10.1080/08941920.2021.1900963
795 Powers, N.C., Wallgren, H.R., Marbach, S., Turner, J.W., 2020. Relationship between Rainfall,
796 Fecal Pollution, Antimicrobial Resistance, and Microbial Diversity in an Urbanized
797 Subtropical Bay. Appl. Environ. Microbiol. 86, 1–15.
798 Rible, J.M., Quick, J., 1960. Method S-19.0. Cation exchange capacity. In: Water soil plant
799 tissue. Tentative methods of analysis for diagnostic purposes, in: Water Soil Plant Tissue.
800 Tentative Methods of Analysis for Diagnostic Purposes. Mimeographed Report, Davis, CA.
801 Roosa, S., Wattiez, R., Prygiel, E., Lesven, L., Billon, G., Gillan, D.C., 2014. Bacterial metal
802 resistance genes and metal bioavailability in contaminated sediments. Environ. Pollut. 189,

143–151. https://doi.org/10.1016/J.ENVPOL.2014.02.031
Rottle, N.D., 2018. From the household to watershed: A cross-scale analysis of residential intention to adopt green stormwater infrastructure. Landsc. Urban Plan. 180, 195–206. https://doi.org/10.1016/j.landurbplan.2018.09.005
Rottle, N.D., 2013. Urban green infrastructure for climate benefit: global to local. Nord. J. Archit. Res. 25, 43–66.
RStudio Team, Rs., 2020. RStudio: Integrated Development for R [WWW Document].
Sanders, B.F., Grant, S.B., 2020. Re-envisioning stormwater infrastructure for ultrahazardous flooding. WIREs Water 7, 1–13. https://doi.org/10.1002/wat2.1414
Sansalone, J.J., Buchberger, S.G., 1997. Partitioning and First Flush of Metals in Urban Roadway Storm Water. J. Environ. Eng. 123, 134–143. https://doi.org/10.1061/(asce)0733-9372(1997)123:2(134)
Schlüter, A., Heuer, H., Szczepanowski, R., Forney, L.J., Thomas, C.M., Pühler, A., Top, E.M., 2007. The 64 508 bp IncP-1b antibiotic multiresistance plasmid pB10 isolated from a waste-water treatment plant provides evidence for recombination between members of different branches of the IncP-1b group. https://doi.org/10.1099/mic.0.26570-0
Seiler, C., Berendonk, T.U., 2012. Heavy metal driven co-selection of antibiotic resistance in soil and water bodies impacted by agriculture and aquaculture. Front. Microbiol. 3, 399. https://doi.org/10.3389/fmicb.2012.00399
Sheldrick, B.H., Wang, C., 1993. Particle-size distribution. Soil Sampling and Methods of Analysis, Canadian Society of Soil Science, Lewis Publishers, Ann Arbor, MI.
Sidhu, J.P.S., Hodgers, L., Ahmed, W., Chong, M.N., Toze, S., 2012. Prevalence of human pathogens and indicators in stormwater runoff in Brisbane, Australia. Water Res. 46, 6652–6660. https://doi.org/10.1016/j.watres.2012.03.012
Singer, A.C., Shaw, H., Rhodes, V., Hart, A., 2016. Review of antimicrobial resistance in the environment and its relevance to environmental regulators. Front. Microbiol. 7, 1–22. https://doi.org/10.3389/fmicb.2016.01728
Smith, D.B., Cannon, W.F., Woodruff, L.G., Solano, F., Kilburn, J.E., Fey, D.L., 2013. Geochemical and mineralogical data for soils of the conterminous United States. Reston, Virginia. https://doi.org/10.3133/ds801
Stepanauskas, R., Glenn, T.C., Jagoe, C.H., Tuckfield, R.C., Lindell, A.H., King, C.J., McArthur, J. V., 2006. Coselection for microbial resistance to metals and antibiotics in

freshwater microcosms. Environ. Microbiol. 8, 1510–1514. https://doi.org/10.1111/j.1462-2920.2006.01091.x

Su, H.C., Pan, C.G., Ying, G.G., Zhao, J.L., Zhou, L.J., Liu, Y.S., Tao, R., Zhang, R.Q., He, L.Y., 2014. Contamination profiles of antibiotic resistance genes in the sediments at a catchment scale. Sci. Total Environ. 490, 708–714. https://doi.org/10.1016/j.scitotenv.2014.05.060

Templ, M., Filzmoser, P., Reimann, C., 2008. Cluster analysis applied to regional geochemical data: Problems and possibilities. Appl. Geochemistry 23, 2198–2213. https://doi.org/10.1016/j.apgeochem.2008.03.004

Tessier, A., Campbell, P.G.C., Bisson, M., 1979. Sequential Extraction Procedure for the Speciation of Particulate Trace Metals. Anal. Chem. 51, 844–851. https://doi.org/10.1021/ac50043a017

U.S. Department of Agriculture, 1998. Soil Quality Information Sheet, European Journal of Soil Biology. https://doi.org/10.1016/S1164-5563(01)01111-6

U.S. Environmental Protection Agency, 1996. Method 3050B: Acid digestion of sediments, sludges, and soils., 1996. Washington, DC. https://doi.org/10.1117/12.528651

UC Office of the President, 2016. UC awards $17M in grants for critical, innovative research. Univ. Calif. Press Room.

Violante, A., Cozzolino, V., Perelomov, L., Caporale, A.., Pigna, M., 2010. Mobility and Bioavailability of Heavy Metals and Metalloids in Soil Environments. J. soil Sci. plant Nutr. 10, 268–292. https://doi.org/10.4067/S0718-95162010000100005

Wang, F., Stedtfeld, R.D., Kim, O.S., Chai, B., Yang, L., Stedtfeld, T.M., Hong, S.G., Kim, D., Lim, H.S., Hashsham, S.A., Tiedje, J.M., Sul, W.J., 2016. Influence of soil characteristics and proximity to antarctic research stations on abundance of antibiotic resistance genes in soils. Environ. Sci. Technol. 50, 12621–12629. https://doi.org/10.1021/acs.est.6b02863

Wang, H., Yilihamu, Q., Yuan, M., Bai, H., Xu, H., Wu, J., 2020. Prediction models of soil heavy metal(loid)s concentration for agricultural land in Dongli: A comparison of regression and random forest. Ecol. Indic. 119. https://doi.org/10.1016/j.ecolind.2020.106801

Wang, Q., Liu, L., Hou, Z., Wang, L., Ma, D., Yang, G., Guo, S., Luo, J., Qi, L., Luo, Y., 2020. Heavy metal copper accelerates the conjugative transfer of antibiotic resistance genes in freshwater microcosms. Sci. Total Environ. 717, 137055.

https://doi.org/10.1016/j.scitotenv.2020.137055
Zhang, F., Zhao, X., Li, Q., Liu, J., Ding, J., Wu, H., Zhao, Z., Ba, Y., Cheng, X., Cui, L., Li, H., Zhu, J., 2018. Bacterial community structure and abundances of antibiotic resistance genes in heavy metals contaminated agricultural soil. Environ. Sci. Pollut. Res. 25, 9547–9555. https://doi.org/10.1007/s11356-018-1251-8
Zhao, Z., Wang, J., Han, Y., Chen, J., Liu, G., Lu, H., Yan, B., Chen, S., 2017. Nutrients, heavy metals and microbial communities co-driven distribution of antibiotic resistance genes in adjacent environment of mariculture. Environ. Pollut. 220, 909–918. https://doi.org/10.1016/j.envpol.2016.10.075
Zhou, S.Y.D., Zhang, Q., Neilson, R., Giles, M., Li, H., Yang, X.R., Su, J.Q., Zhu, Y.G., 2021. Vertical distribution of antibiotic resistance genes in an urban green facade. Environ. Int. 152. https://doi.org/10.1016/j.envint.2021.106502

Graphical Abstract